Role of Molecular Structure on the Thermodynamic Properties of Melts, Blends, and Concentrated Polymer Solutions. Comparison of Monte Carlo Simulations with the Cluster Theory for the Lattice Model

Jacek Dudowicz and Karl F. Freed*

James Franck Institute and Department of Chemistry, The University of Chicago, Chicago, Illinois 60637

William G. Madden

Central Research and Development and Polymer Products Departments, E. I. du Pont de Nemours and Company, Experimental Station, Wilmington, Delaware 19880

Received December 22, 1989; Revised Manuscript Received March 23, 1990

ABSTRACT: Approximate lattice model treatments of the energies of mixing and coexistence curves of polymer solutions and melts are compared against Monte Carlo simulations of these properties for the same lattice model. Because the comparisons do not involve adjustable parameters, they represent stringent tests of lattice theories of polymer fluids. The theories considered are those due to Flory, Huggins, and Guggenheim and the recent cluster theory of Freed and co-workers. A new purely algebraic derivation of the latter method, briefly sketched previously, is provided, and additional calculations are performed to extend and correct prior results for polymer solutions, melts, and incompressible blends. The comparison with Monte Carlo simulations for the polymer–solvent (or isomorphic polymer-void) system shows the present cluster theory to produce the most accurate treatment of the energies of mixing and coexistence curves for this system. Given this good agreement between the lattice cluster theory and Monte Carlo calculations for the same lattice model, cluster theory computations are provided for the exhibition of the predicted strong variation of these thermodynamic properties with monomer and solvent molecular structures.

1. Introduction

Theoretical descriptions of thermodynamic properties of polymer blends, melts, and concentrated solutions require the introduction of models to capture the salient physical features of these complicated fluids.[1,2] For instance, the exact monomer–monomer and monomer–solvent interaction potentials are not known, and consequently idealized models are introduced. These models may, for example, use pairwise additive monomer–monomer and monomer–solvent interactions, while in reality such interactions most likely contain nonpairwise additive and highly orientation-dependent contributions. Alternative models place monomers and solvent molecules on a lattice. Despite the simplifying nature of these models, the statistical mechanical treatment of even these idealized models of polymeric fluids is very complicated, and, therefore, approximations are required. The necessity for approximations leads to difficulties in comparing theoretical predictions with experimental data: First of all, it is possible that the exact solution of a model would adequately represent the data but that the approximations used in treating the model introduce inaccuracies, which result in poor agreement with experiment. It is also possible that the combination of an inadequate model with approximations in its solution could produce predictions that are in fortuitous accord with experiment. Evidently, the interpretation of the accuracy of a model and its implications for the interpretation of experimental data require the differentiation between the quality of the statistical mechanical model and the quality of the mathematical solution of that model.

It is useful to recognize the difference between statistical mechanical models, which are defined by an explicit representation for the configurational potential energy (or its equivalent), and the wider class of phenomenological models[3,4] for which some parameters cannot be evaluated from the configurational energy of the model. The former have, in principle, exact solutions, which may be compared with Monte Carlo simulations of the identical model while the latter cannot. Monte Carlo simulations continue to be extremely useful in testing the accuracy of approximate treatments of statistical mechanical models and thereby in paving the way toward improved approximations. Subsequent comparisons with experiment indicate the limitations inherent in the models and thereby enable the generation of improved models.

A previous paper by Madden et al.[5] employs Monte Carlo simulations of lattice polymer–solvent systems to assess the accuracy of approximate solutions of the same model by Pesci and Freed[6,7] for describing the internal energies of mixing and the coexistence curves. The Pesci–Freed[6] calculations solve the standard lattice model of interacting polymer–solvent systems by using a double expansion in powers of z^{-1}, where z is the lattice coordination number, and of ϵ/kT, where ϵ is the effective polymer–solvent interaction energy [see (2.1) below] and kT is the thermal energy. Their calculations of the order of ϵ/kT contribution (the first-order energy) are in good agreement with the Monte Carlo computations, while inaccuracies appear in higher order contributions in ϵ/kT. Despite the accuracy of the first-order energy and that of the athermal entropy of mixing (as previously demonstrated by comparisons with Monte Carlo calculations of Dickman and Hall[8]), the Pesci–Freed computations provide a rather poor representation of the coexistence curve, and this has led to a reinvestigation of the approximations inherent in the analytical cluster expansion computations.

The theory of corrections to the classic Flory–Huggins approximation[9,10] for the lattice model of interacting polymer–solvent systems represents the corrections in terms of a cluster expansion that bears strong similarities to that of Mayer for the description of nonideal gases.[11]

0024-9297/90/2223-4803$02.50/0

The coefficients of individual powers of z^{-1} have contributions from several Mayer-like cluster diagrams, and Pesci–Freed have retained only the leading portion of these diagrams in an additional expansion in inverse powers of the polymerization index M. While the errors so incurred in the athermal limit for the energy of mixing are of the expected order of a few percent, subtle cancellations between leading and subdominant terms in M from different diagrams produce gross inaccuracies in small chemical potentials and hence in the computed coexistence curve.

Lattice model calculations are performed here for the first-order energy through order z^{-2} corrections, for the second-order energy through order z^{-1} corrections, and for the leading third- and fourth-order energies, without the use of any simplifying additional approximations. The calculations are made for hypercubic lattices in d dimensions for which $z = 2d$. Treatment of other lattices is possible, and the interesting case of $d = 2$ may converge more slowly and therefore require additional terms in the z^{-1} expansion. The present lattice cluster theory calculations display improved agreement with the $d = 3$ Monte Carlo simulations, and the first-order energies are numerically quite close to the energy produced by the Guggenheim random-mixing (GRM) approximation[3,12] (as are the mixing entropies). The coexistence curves obtained from the first-order (in ϵ) cluster theory and GRM are likewise now in close agreement, but both have significant differences with the simulations. The origins of these differences are investigated here within the cluster expansions by computing the first correction (in the z^{-1} expansion) to the order ϵ^2 contributions along with the leading parts of the ϵ^3 and ϵ^4 order terms in the energy of mixing.

Because of the accurate agreement between the present theory and the Monte Carlo simulations for the same model, we also provide theoretical computations of the role of monomer and solvent structure on both the energies of mixing and coexistence curves. Whereas the available Monte Carlo simulations are currently limited to linear-chain models of both the polymer and solvent molecules, the lattice theory formulation applies to a wide variety of models in which the monomers and/or the solvent molecules are allowed to have internal structures with a particular architecture and therefore to occupy several neighboring lattice sites. Thus, we apply the lattice theory in an investigation of the thermodynamic implications of monomer and solvent molecular structure.

Section 2 provides an algebraic derivation of the cluster expansion for packing entropies that is only briefly outlined in the review by Freed and Bawendi.[13] The algebraic derivation of the van der Waals interaction energies is developed here for the first time and provides several simplifications in the derivation of diagram rules and in the computational scheme that is described in more detail in the Appendix. Particular focus is placed on the treatment of the leading order ϵ^3 and ϵ^4 contributions, which are first evaluated here. Results are provided for the order z^{-1} corrections to the ϵ^2 terms, but the lengthy calculational details will be presented elsewhere. Some discussion is provided of the subtle cancellation of terms between and within the energy diagrams. While the Monte Carlo simulations pertain to the polymer–solvent (or polymer-void) system, the analytical expressions are presented both for this system and for the incompressible binary polymer blend, since the former system merely follows as a special case of the latter. A detailed description of the blends is likewise left for a future work. Section 4 presents the comparisons between the cluster theory, earlier approximations to the standard lattice model, and the Monte Carlo calculations for energies of mixing and for coexistence curves. The details of the Monte Carlo simulation methods are thoroughly described in ref 5 and references therein along with the simulation data and tests of the pseudokinetic method used. Thus, we merely quote the simulation data in our tests of the various theories. We also use the cluster theory here to consider the variation in thermodynamic quantities that arises for polymers with structured monomers and/or structured solvent molecules.

2. Lattice Model and Cluster Expansion for Packing Entropies

The standard lattice model takes monomers and solvent molecules to lie at the point sites of a regular array. Each lattice site may be occupied by either a monomer or a solvent molecule, and there is a strict prohibition against multiple occupancy of a lattice site. The polymer chains are represented by sequences of $N - 1$ bonds between the consecutive monomers on the chains. Lattice sites have z nearest neighbors, giving z possible directions for the bonds emanating from a given lattice site. van der Waals attractive energies ϵ_{pp}, ϵ_{ss}, and ϵ_{ps} are present between nearest-neighbor monomers, solvent molecules, and monomer–solvent pairs. For the purposes of comparison with Monte Carlo calculations, all lattice sites are taken to be occupied, and consequently there is but a single interaction energy ϵ that appears in excess thermodynamic properties.[14]

$$\epsilon = (\epsilon_{pp} + \epsilon_{ss} - 2\epsilon_{ps}) \tag{2.1}$$

More generally, it is possible to allow the system to be compressible and model the free volume by the presence of lattice sites that are unoccupied by either monomers or solvent molecules, and this generalization will be considered in future work as it is necessary to describe equations of state of, for instance, polymer blends.

Nemirovsky et al.[15] have introduced a generalization of this standard lattice model in which the individual monomers (and/or solvent molecules) have detailed structures, so each monomer (and/or solvent molecule) occupies several lattice sites, where the submonomer units on different lattice sites are connected by flexible bonds as depicted in Figure 1. Such a generalization more faithfully represents the actual molecular structure. However, simple approximations to the lattice model, such as the classic Flory–Huggins approximation, do not distinguish between the different chain architectures depicted in Figure 1, and consequently this generalized model is useful if sufficient corrections are appended to the Flory–Huggins approximation.[9,10] These corrections may be evaluated by using the cluster expansion methods described briefly below and in previous references.[6,15-17] Since the Monte Carlo simulations are currently available for linear-chain models of the polymer, we continue to discuss the cluster expansion method with reference to linear-chain polymers and solvent molecules that each occupy a single lattice site, but the final results are quoted in a general form that is applicable to arbitrary chain architectures. In fact, the calculations are performed quite generally for an incompressible blend of two different polymers of arbitrary architectures. The polymer–solvent system is but a special limit of a blend in which one of the chains is quite short. A given chain architecture may be represented by a linear sequence or a complicated branching pattern in which the monomers have specified structures. However, all chains of a given architecture are

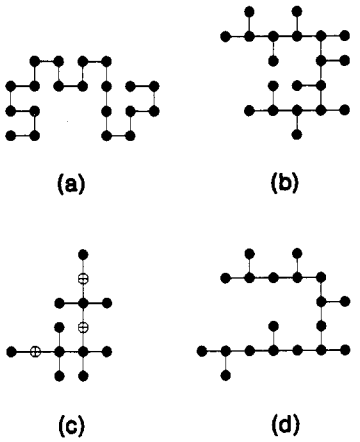

Figure 1. Sample of four polymer architectures. Structures (a)–(c) represent three different polymer chains with the same segment number $M = 20$ but different architectures and different number N of bonds in the chain backbone. Structures (a)–(c) have $N = 19$, 10, and 7, respectively. Chains are drawn in two dimensions, for simplicity. A circle with crossed bars designates that there are two bonds emanating from the site in opposite directions, perpendicular to the plane of the figure. Structure (d) is a more sparsely branched version of (b) and is displayed here for $M = 19$ and $N = 12$.

considered to have the same bonding topology and not to have small closed loops. Treating such irregular structured chains (or lightly cross-linked networks) requires only the specification of certain counting indices, described below.

The original derivation[16,17] of the cluster expansion for corrections to the Flory–Huggins approximation uses field theoretic methods, which are generally unfamiliar to polymer scientists. Recent work by Freed and Bawendi[13] briefly sketches the beginnings of a new derivation employing familiar mathematical methods. Below we provide a more detailed version of the formulation that extends well beyond the sketch previously given.

A. Analytic Representation of the Lattice Model. To introduce some notation, let $\mathbf{a}_\beta$, $\beta = 1, ..., z$ designate the vectors from a given lattice site to the z nearest-neighbor lattice sites and let $\mathbf{r}_i$ denote the position of the ith lattice site with respect to the origin of coordinates. The condition that the lattice sites i and j are nearest neighbors is just

$$\mathbf{r}_i = \mathbf{r}_j + \mathbf{a}_\beta \quad \text{for some } \beta = 1, ..., z \tag{2.2}$$

Thus, the constraint that sites i and j are nearest neighbors may be introduced by use of the Kronecker delta

$$\delta(\mathbf{r}_i,\mathbf{r}_j+\mathbf{a}_\beta) \equiv \delta(i,j+\beta) \tag{2.2a}$$

where the right-hand side of (2.2a) is used as a shorthand notation.

It is now straightforward to use the notation (2.2) in representing the bonding constraints for a set of n_p linear polymers with $N - 1$ bonds each. The first bond on the first chain enters into our counting scheme with the factor of $\sum_{\beta_1}\delta(i_1^1,i_2^1+\beta_1^1)$, where the superscript labels the chain number, the subscript labels the sequential monomer numbering along the chain, and the bond in question may be in any of the z different possible orientations. The next bond has the obvious weight factor of $\sum_{\beta_2}\delta(i_2^1,i_3^1+\beta_2^1)$ with the added excluded-volume constraint that sites $i_3^1 \neq i_1^1$, etc. Continuing this process for all bonds and all chains and introducing a factor of $(n_p!)^{-1}$ to account for the indistinguishability of all chains and the symmetry number of $^1/_2$ for each chain, the partition function for packing n_p monodisperse linear polymers of polymerization index N is written as

$$W(n_p,N) = \frac{1}{n_p!2^{n_p}} \sum_{\substack{i_1^1\neq i_2^1\neq ...\neq i_N^1 \\ \neq i_1^2\neq i_2^2\neq ...\neq i_N^2 \\ \neq i_1^{n_p}\neq i_2^{n_p}\neq ...\neq i_N^{n_p}}} \prod_{m=1}^{n_p}\{\prod_{\alpha=1}^{N-1}\sum_{\beta_\alpha^m=1}^{z}\delta(i_\alpha^m,i_{\alpha+1}^m+\beta_\alpha^m)\} \tag{2.3}$$

The complexity in evaluating (2.3), of course, stems from the excluded-volume constraint on the summation that prohibits any two monomers from occupying the same lattice site. The excluded-volume constraint, $i_\alpha^m \neq i_{\alpha+1}^m$, between successively bonded monomers has been inserted into (2.3) both for notational symmetry and for computational reasons. The Kronecker delta functions in (2.3) prohibit bonded monomers from occupying the same lattice site. However, in the developments below, these strict bonding constraints are only treated approximately, so the imposition of the $i_\alpha^m \neq i_{\alpha+1}^m$ condition for all α and m in (2.3) is then no longer redundant and ensures that excluded-volume constraints are still preserved within the approximation scheme. Equation 2.3 is an exact representation of the lattice model for d-dimensional hypercubic lattices in the athermal limit.

B. Exact Formal Solution and Flory–Huggins Approximation. The Flory mean-field approximation replaces the exact bonding constraints in (2.3) (the Kronecker delta functions) by crude averages.[9] In order to extract this average (or mean-field) contribution and to enable the systematic computation of corrections, it is useful to transform (2.3) in a fashion that at first sight might appear to make it look more complicated. To this end, we now introduce for each Kronecker delta in (2.3) the lattice identity

$$\delta(i,j+\beta) = N_l^{-1}\sum_{\mathbf{q}} \exp[i\mathbf{q}\cdot(\mathbf{r}_i - \mathbf{r}_j - \mathbf{a}_\beta)] \tag{2.4}$$

where N_l is the number of lattice sites and the summation runs over the first Brillouin zone. For instance, on three-dimensional hypercubic lattices this Brillouin zone contains the $\mathbf{q}$ vectors specified by $q_x = 2\pi n_x/a_x$ and $n_x = 0, 1, 2, ..., N_l^{1/3} - 1$, etc., for q_y and q_z. The αth bond on the mth chain thus involves the wave vector summation index $\mathbf{q}_\alpha^m$.

Since there are z possible directions β for each bond, the sum over β of (2.3) may be decomposed as

$$\sum_\beta \delta(i,j+\beta) = \frac{z}{N_l}\left\{1 + \frac{1}{z}\sum_{\mathbf{q}\neq 0} f(\mathbf{q})\exp[i\mathbf{q}\cdot(\mathbf{r}_i - \mathbf{r}_j)]\right\} \tag{2.5}$$

where the $\mathbf{q} = 0$ term is explicitly given by the first term on the right-hand side of (2.5) and where $f(\mathbf{q})$ is the nearest-neighbor structure factor

$$f(\mathbf{q}) = \sum_{\beta=1}^{z}\exp(-i\mathbf{q}\cdot\mathbf{a}_\beta) \tag{2.6}$$

Using (2.5) for each Kronecker delta in (2.3) converts the latter into

$$W(n_p,N) = \frac{1}{n_p!2^{n_p}}\sum_{i_1^1\neq ...\neq i_N^{n_p}}\prod_{m=1}^{n_p}\prod_{\alpha=1}^{N-1}\left(\frac{z}{N_l}\right)\times \left\{1 + \frac{1}{z}\sum_{\mathbf{q}_\alpha^m\neq 0} f(\mathbf{q}_\alpha^m)\exp[i\mathbf{q}_\alpha^m\cdot(\mathbf{r}_{i_\alpha}^m - \mathbf{r}_{i_{\alpha+1}}^m)]\right\} \tag{2.7}$$

which is another exact algebraic representation of the n_p polymer packing problem. The product over α and m in

(2.7) is of the form

$$W(n_p,N) = \frac{1}{n_p!2^{n_p}} \sum_{i_1{}^1 \neq \ldots \neq i_N{}^{n_p}} \prod_{m=1}^{n_p} \prod_{\alpha=1}^{N-1} \left[\frac{z}{N_l}(1 + X_{\alpha,m}) \right] \tag{2.8a}$$

with each polymer bond α,m providing the correlation term

$$X_{\alpha,m} = \frac{1}{z} \sum_{\mathbf{q}_\alpha{}^m \neq 0} f(\mathbf{q}_\alpha{}^m) \exp[i\mathbf{q}_\alpha{}^m \cdot (\mathbf{r}_{i_\alpha}{}^m - \mathbf{r}_{i_{\alpha+1}}{}^m)] \tag{2.8b}$$

As discussed below, the product form of (2.8) naturally generates a cluster expansion in much the same way as in Mayer's cluster expansion for the statistical mechanics of nonideal gases.[11]

The leading contribution arises from the factor of unity in (2.8a) for each α and m and yields the mean-field approximation

$$W^{MF}(n_p,N) = \frac{1}{n_p!2^{n_p}} \sum_{i_1{}^1 \neq \ldots \neq i_N{}^{n_p}} \prod_{m=1}^{n_p} \prod_{\alpha=1}^{N-1} \left(\frac{z}{N_l} \right) \tag{2.9}$$

The summand in (2.9) no longer depends on the monomer positions (the $\mathbf{r}_{i_\alpha}{}^m$), and thus (2.9) corresponds to Flory's approximation in which all monomer correlations, due to the contributions to (2.7) from the $f(\mathbf{q}_\alpha{}^m)$ terms, are ignored. Because of this absence of correlations, the summation in (2.9) is readily evaluated as

$$W^{MF}(n_p,N) = \frac{1}{n_p!2^{n_p}} \frac{N_l!}{(N_l - n_pN)!} \left(\frac{z}{N_l} \right)^{n_p(N-1)} \tag{2.10}$$

Equation 2.10 recovers the classic Flory–Huggins combinatorial packing entropy for the n_p polymers, while its generalization to blends provides the corresponding Flory–Huggins entropy for this system.[18] The remaining terms from the cluster expansion in (2.7), therefore, produce the corrections to the Flory–Huggins approximation as arising from correlations, neglected entirely by Flory,[9] between the placement of monomers and bonds on the lattice.

C. Cluster Expansion for Packing Entropies. The quantities $X_{\alpha,m}$ in (2.8b) depend on the explicit positions of the two segments forming the αth bond on the mth polymer chain, and thus the $X_{\alpha,m}$ represent the corrections arising from correlations in monomer positions. Expanding the product in (2.8a) leads to a cluster expansion of the form

$$1 + \sum_{\alpha,m} X_{\alpha,m} + \sum_{\alpha,m>\alpha',m'} X_{\alpha,m}X_{\alpha',m'} + \ldots \tag{2.11}$$

where the designation $\alpha,m > \alpha',m'$ indicates that the summation in (2.11) runs over all distinct pairs of bonds. The linear terms in $X_{\alpha,m}$ are called the one-bond contributions; the quadratic are the two-bond contributions, etc. When substituted into (2.7), the leading term of unity in (2.11) generates the leading, Flory approximation of (2.10), while the remainder of (2.11) produces, respectively, the correlated one-bond, two-bond, ... contributions to the cluster expansion. The summation over distinct lattice sites in (2.7) runs over those lattice sites connected by the correlating bonds, as indicated in the summation indices of (2.11), along with the remaining lattice sites, which are either unoccupied or have uncorrelated monomers. Summation over vacant or uncorrelated sites is trivial and gives a combinatorial factor of $[(N_l - n_v)!]/[(N_l - n_pN)!]$, where n_v is the number of lattice sites connected by the correlating bonds [i.e., associated with the summation indices α,m, α',m', ... in (2.11)]. For instance, the Flory term has $n_v = 0$, and the sum involves the restriction to $i_1{}^1 \neq \ldots \neq i_N{}^{n_p}$. Likewise, when (2.11) is inserted into (2.8a), each one-bond contribution (i.e., each $X_{\alpha,m}$) contributes identically, so the summation $\sum_{\alpha,m}$ in the resultant equation yields the number of bonds $n_p(N - 1)$ in the system. The next summation $\sum_{\alpha,m>\alpha',m'}$ again has identical contributions from all pairs of bonds, but the value of the summation over the $i_\alpha{}^m$ depends on whether the bonds lie on the same or different chains. The resulting cluster expansion for the partition function (2.7) is identical with the one derived previously[16,17] by using more lengthy and less familiar field theoretic methods.

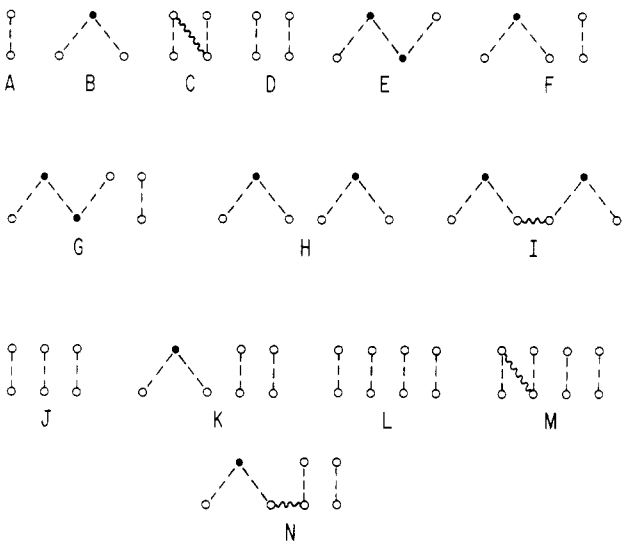

Figure 2. Diagrams used to calculate entropic corrections to Flory–Huggins packing entropy of linear chains to order z^{-2} and N_l. The symbols used in the diagramatic expansion follow those from refs 15 and 18. Additional diagrams corresponding to branched chains can be found in ref 15.

The lattice polymer packing entropy cluster expansion is depicted diagrammatically in Figure 2, where straight lines represent the correlating bonds. Diagram A of Figure 2 corresponds to the one-bond contribution from (2.11) and (2.7), while diagrams B–D are the two-bond terms. The two correlating bonds in D lie on different polymer chains, and those in B lie sequentially along a single polymer chain, while those in C lie nonsequentially along one chain (with one or more uncorrelated intervening monomers). Some three- and four-bond diagrams for linear chains are also presented in Figure 2. The rules for constructing the diagrams and evaluating their contributions are summarized in Nemirovsky et al.[15] and references therein, so they are not repeated here. In addition, Nemirovsky et al. describe how the theory can be generalized to branched polymer architectures, composed of structured monomers. The details are not repeated here, except as necessary to evaluate some new energy contributions. Although Nemirovsky et al. provide the structured monomer generalization using field theoretic methods, they can more easily be obtained with the current algebraic approach. For instance, a solvent molecule structure with one central unit connected by flexible bonds to four other units contributes to the partition function a factor of

$$W(1,\text{tetra}) = \sum_{i \neq i_1 \neq i_2 \neq i_3 \neq i_4} \prod_{\alpha=1}^{4} \sum_{\beta_\alpha=1}^{z} \delta(i,i_\alpha+\beta_\alpha) \tag{2.12}$$

with extension to the structures in Figure 1 rather straightforward.

Bawendi et al.[17] explain that the packing cluster expansion given diagrammatically in Figure 2 can be represented as a series expansion in z^{-1}, where the

evaluation of contributions through order z^{-n} requires retention of all diagrams having up to $2n$ bonds. Branched structures, such as those in Figure 1, may be distinguished from linear ones by considering at least three correlating bonds that meet at a common junction. Thus, we perform the packing calculations to order z^{-2} to include the leading contributions distinguishing monomer architectures. Comparisons of computed packing entropies to order z^{-2} for linear chains are found to agree well with Monte Carlo simulations,[8] and similar comparisons for branched structures are desirable. Unfortunately, branching probably leads to greater complexity in some simulation methods.

Packing entropies of athermal limit polymers are obtained from the Boltzmann definition

$$S(n_p,N) \equiv k \ln W(n_p,N) = k \ln W^{MF}(n_p,N) + k \ln [1 + \sum_B \gamma_D D_B] \quad (2.13)$$

where the notation of Nemirovsky et al. is employed to represent the corrections to the Flory–Huggins approximation in terms of a summation of contributions from cluster diagrams. Each diagram contains B correlating bonds, and its value may be decomposed into the product of a monomer structure-dependent combinatorial factor, γ_D, and a monomer structure-independent diagram value, D_B. Rules for computing these quantities are given in previous papers and are discussed below in reference to the evaluation of the new energy contributions. In the leftmost term in (2.13) it is understood that the logarithm is expanded in a Taylor series, whose contributions are collected into cumulants.[15,19] This process is necessary in order to handle the following perverse character of the lattice polymer cluster expansion: Diagrams D, F, G, etc. of Figure 2 are disconnected diagrams, which contain two sets of correlating bonds that are unconnected by correlating bonds. In contrast to the majority of other cluster expansions, the value of these disconnected diagrams is not related to the products of the values of the disconnected portions, in part because of the excluded-volume constraints on the summation of (2.7) requiring that all monomers in the disconnected diagram fragments lie on distinct lattice sites. The construction of cumulants serves to cancel all higher than extensive contributions, leaving only an extensive free energy.

The expansion of the packing entropy to order z^{-2} is given by Bawendi and Freed[18] for linear polymer–solvent and linear polymer–polymer systems, but the extension to structured monomers in ref 6 contains the errors noted in the introductioin. Hence, the corrected expressions for the athermal limiting entropy of mixing, ΔS_∞^{mix}, for incompressible two-component systems are given in Table I. These expressions apply to polymer blends, to polymer–solvent systems, and to binary mixtures of small-molecule liquids. Monomers and solvent molecules may have structures that cover several lattice sites. In order to conform to the notation of Nemirovsky et al.[15] describing structured monomers, the chains are now taken to have N bonds along the chain backbone and to cover M lattice sites per chain. The structure dependence in Table I enters through the combinatorial numbers $N_i^{(l)}$ that describe the architecture of species l. Values of the $N_i^{(l)}$ for polymers with the structures in Figure 1 are presented in Table I of Nemirovsky et al., while generalization to other architectures results from the definitions of the $N_i^{(l)}$ as follows: N_i is the number of sequential sets of i bonds in a polymer that covers M sites; $N_{i,j}$ is the number of nonsequential sets of i and j bonds,

Table I
Noncombinatorial Athermal Limit of Entropy of Mixing for a Binary Incompressible Blend ($\phi_1 + \phi_2 = 1$)[a]

$$\frac{-\Delta S_\infty^{mix} - \frac{\phi_1}{M_1}\ln\phi_1 - \frac{\phi_2}{M_2}\ln\phi_2}{kN_l\phi_1\phi_2} = \frac{1}{z}A_1^2 + \frac{1}{z^2}[\sum_{i=2}^{12} A_i + \phi_1 \sum_{i=13}^{16} A_i + \phi_1^2 A_{17}]$$

$A_1 = N(1,1) - N(1,2)$
$A_2 = -4A_1[N(2,1) - N(2,2)]$
$A_3 = A_{13} = (8/3)(A_1)^3$
$A_4 = 8(A_1)^2N(1,2)$
$A_5 = -2A_1[N(3,1) - N(3,2)]$
$A_6 = [N(2,1) - N(2,2)]^2$
$A_7 = -2A_1[[N(1,2;1) - N(1,1)N(2,1)M_1] - [N(1,2;2) - N(1,2)N(2,2)M_2]]$
$A_8 = A_{14} = A_{17} = 2(A_1)^4$
$A_9 = 4[A_1N(1,2)]^2$
$A_{10} = 8(A_1)^2N(1,1)N(1,2)$
$A_{11} = 2A_1[[N(1,1) + N(1,2)][N(1,1;1) - N(1,1)^2M_1] - 2N(1,2)[N(1,1;2) - N(1,2)^2M_2]]$
$A_{12} = -6A_1[N(\perp,1) - N(\perp,2)]$
$A_{15} = (A_1)(A_4)$
$A_{16} = 2(A_1)^2[[N(1,1;1) - N(1,1)^2M_1] - [N(1,1;2) - N(1,2)^2M_2]]$

[a] $N(\alpha,l) \equiv N_\alpha^{(l)}/M_l$, $l = 1$ and 2; $N(\alpha,\beta;l) \equiv N_{\alpha,\beta}^{(l)}/M_l$, $l = 1$ and 2.

Table II
Noncombinatorial Athermal Limit of Entropy of Mixing for a Polymer-Void (Solvent) System[a]

$$\frac{-\Delta S_\infty^{mix} - \frac{\phi}{M}\ln\phi - (1-\phi)\ln(1-\phi)}{kN_l\phi(1-\phi)} = \frac{1}{z}A_1^2 + \frac{1}{z^2}[\sum_{i=2}^{9} A_i + \phi \sum_{i=10}^{12} A_i + \phi^2 A_{13}]$$

$A_1 = N(1)$
$A_2 = -4A_1N(2)$
$A_3 = A_{10} = (8/3)(A_1)^3$
$A_4 = -2A_1N(3)$
$A_5 = [N(2)]^2$
$A_6 = -2A_1[N(12) - N(1)N(2)M]$
$A_7 = A_{11} = A_{13} = 2(A_1)^4$
$A_8 = A_{12} = 2(A_1)^2[N(11) - [N(1)]^2M]$
$A_9 = -6A_1N(\perp)$

[a] $N(\alpha) \equiv N_\alpha/M$; $N(\alpha\beta) \equiv N_{\alpha,\beta}/M$.

$N_\perp$ is the number of ways in which three bonds meet at a lattice site for a polymer chain, etc. (The definitions of $N_{i,i}$ in ref 15 do not include the symmetry number of $^1/_2$, which is, however, properly included in the calculated entropies in that paper. Thus, we follow the convention of ref 15 for the $N_{i,i}$.) These structure-specific combinatorial indices are readily evaluated for polymers or solvent molecules with regular repeating or rather irregular architectures. Absolute athermal limit entropies may be obtained from Table I by adding $\varphi_1 s_1 + \varphi_2 s_2$, where $s_i = s_i(\varphi_i=1)$ is the specific entropy of pure component i at unit volume fraction φ_i that is obtained from Nemirovsky et al. with a minor typographical correction and replacing diagrams o and q in Figure 6 of ref 15 by one diagram.

The special case of a polymer solution follows from Table I and results given below by letting M_2 become small. For the sake of explicit comparisons with Monte Carlo simulations, the limit in which each solvent molecule occupies a single lattice site follows as $M_2 = 1$ and all $N_i^{(2)} = N_{i,j}^{(2)} = 0$. The resultant athermal entropy of mixing is provided in Table II. Note that Tables I and II explain the existence of entropic contributions to the Flory χ parameter that have entered into previous theories of polymer fluids only as an empirical parameter of uncertain molecular origins. Thus, Tables I and II enable the study

of the relationship between polymer and solvent structure to the properties of this entropic χ for both concentrated polymer solutions and blends. A recent application of the lattice cluster theory considers the cross-link density dependence of χ for swollen polymer networks.[20] We now turn to a consideration of the energetic contributions that are also present in general polymeric fluids.

3. Interaction Energies

As is well-know, the actual interactions in polymer fluids involve both short-range repulsions (which are modeled in Section 2 by the excluded-volume constraints) and longer range attractive interactions. This section considers the introduction of the latter interactions into the lattice model. Let $\epsilon_{kl}^{ij} = \epsilon_{kl}$ be a shorthand notation representing the van der Waals attractive energies (in units of kT) that apply when beads of species k and l occupy nearest-neighbor sites i and j on the lattice. Given this notation, the total interaction energy may be written as

$$\exp\Big(\sum_{i\in S_k j\in S_l} \epsilon_{kl}^{ij}\Big) = \prod_{i\in S_k j\in S_l} [1 + \sum_{\beta=1}^{z} \delta(i,j+\beta) f_{kl}] \tag{3.1}$$

where f_{kl} is the Mayer f function

$$f_{kl} = \exp(\epsilon_{kl}) - 1 \tag{3.2}$$

for the interaction between lattice sites occupied by species k and l and S_k designates the set of lattice sites occupied by segments of polymer of species k, etc. The partition function, $Z(n_p,N)$, for the interacting system is obtained by multiplying the right-hand side of (2.3) by the right-hand side of (3.1). The general multicomponent case requires cumbersome bookkeeping, so the final result is presented for the simple case of the polymer–solvent or polymer-void system in which we may use the single effective interaction parameter of (2.1). When S is taken to designate the set of lattice sites $i_1{}^1 \neq \ldots \neq i_N{}^{n_p}$ that are occupied by polymers, this result is

$$Z(n_p,N) = \frac{1}{n_p!2^{n_p}} \sum_{i_1{}^1\neq\ldots\neq i_N{}^{n_p}} \prod_{m=1}^{n_p} \prod_{\alpha=1}^{N-1} \sum_{\beta_\alpha{}^m=1}^{z} \delta(i_\alpha{}^m, i_{\alpha+1}{}^m + \beta_\alpha{}^m) \exp\Big(\sum_{i>j\epsilon S} \epsilon^{ij}\Big) \tag{3.3}$$

The sum over i and j in (3.3) consequently runs over all pairs of lattice sites that are occupied by polymers. Hence, the summation indices in the exponent portion of (3.3) are connected to the overall ones that also appear in the "entropic factor" arising from (2.3).

The Helmholtz free energy, $F(n_p,N)$, is obtained from the partition function, $Z(n_p,N)$, through

$$F(n_p,N) = -kT \ln Z(n_p,N) \tag{3.4}$$

and the free energy of mixing $\Delta F^{mix}(n_p,N) = F(n_p,N) - \varphi_1 F_1 - \varphi_2 F_2$ and the internal energy of mixing $\Delta E^{mix}(n_p,N) \equiv \partial[\Delta F^{mix}(n_p,N)/kT]/\partial[(kT)^{-1}]$ are evaluated in the usual manner. Likewise, all other thermodynamic properties may be evaluated from the free energy.

A. Cluster Expansion. The transformation (2.4) may be applied to all the Kronecker delta functions in $Z(n_p,N)$, and the entropic factor is therefore converted into (2.7). The interaction energy in (3.1) is first expanded in the usual

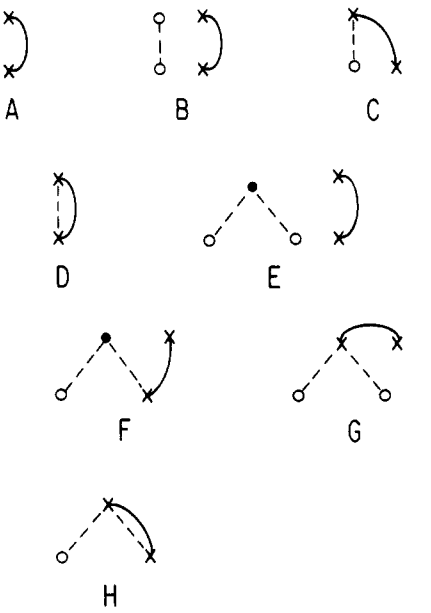

Figure 3. First-order ϵ diagrams used to calculate lowest order corrections in ϵ/kT to Flory–Huggins (mean-field) free energy. Only the first few diagrams are shown as illustration. Following ref 6, curved lines represent the interactions and straight lines represent the correlating bonds.

Mayer expansion

$$\prod_{i>j} [1 + \sum_{\beta=1}^{z} \delta(i,j+\beta) f_{kl}] = 1 + \sum_{\beta=1}^{z} \sum_{i>j} \delta(i,j+\beta) f_{kl} + \sum_{\beta,\beta'=1}^{z} \sum_{i>j\neq i'>j'} \delta(i,j+\beta)\,\delta(i',j'+\beta') f_{kl} f_{k'l'} + \ldots \tag{3.5}$$

Terms in (3.5) are represented diagrammatically by curved lines to distinguish these interaction lines from the correlating bonds of section 2. The diagrammatic representation of the partition function $Z(n_p,N)$ therefore may contain both correlating bonds and interaction lines. As described in refs 6 and 18, the rules for the correlating bonds and interaction lines are quite similar, except that the factors associated with correlating bonds have sums over $\mathbf{q}_\alpha{}^m \neq 0$, while when the identity (2.4) is inserted into individual terms of the expansion (3.5), the interaction lines also contain the $\mathbf{q} = 0$ contributions of z/N_1 from (2.5). It is possible to exploit the compact methods for evaluating these mixed entropy–energy diagrams by following ref 6 and separating the $\mathbf{q} = 0$ from the $\mathbf{q} \neq 0$ contributions from the interaction lines. As described in ref 6, the $\mathbf{q} = 0$ portions cancel extensively among the diagrams and only produce the Flory–Huggins interaction energy, while the $\mathbf{q} \neq 0$ terms provide the corrections to Flory–Huggins. The evaluation of the $\mathbf{q} \neq 0$ parts of the mixed entropy–energy diagrams follows just as for the entropy diagrams apart from the appearance of additional diagrams that have no counterpart in the cluster expansion for athermal limit packing entropies (for example, diagrams D and H of Figure 3). The diagram rules and methods of evaluation emerge just as in ref 6, but here we do not employ the large M approximation to individual diagrams in order to maintain all cancellations. Some of the technical details of these cancellations and of the evaluation of higher terms in the Mayer expansion (3.5) are provided in the Appendix.

B. Results for Polymer Solutions and Blends. Table III presents the free energy and internal energy of mixing for an incompressible binary blend composed of polymers with arbitrary architectures. The table contains the same Nemirovsky et al. counting indices that appear

Table III
Free Energy of Mixing and Internal Energy of Mixing for a Binary Incompressible Blend ($\phi_1 + \phi_2 = 1$)[a]

$$\frac{\Delta F^{mix}}{kTN_l\phi_1\phi_2} = \sum_{i=1}^{4} A_i + \sum_{k,l=1}^{2}\sum_{m} B_m^{(lk)}(1-\delta_{l,k}) + \sum_{k,l=1}^{2}\sum_{m} C_m^{(lk)}(1-\delta_{l,k}) - \frac{\Delta S_\infty^{mix}}{kN_l\phi_1\phi_2}$$

$$\frac{\Delta E^{mix}}{kTN_l\phi_1\phi_2} = \sum_{i=1}^{4} iA_i + \sum_{k,l=1}^{2}\sum_{m} B_m^{(lk)}(1-\delta_{l,k}) + 2\sum_{k,l=1}^{2}\sum_{m} C_m^{(lk)}(1-\delta_{l,k})$$

$$A_1 = \frac{\epsilon z}{2}$$

$$A_2 = -\frac{\epsilon^2 z}{4}\phi_1\phi_2$$

$$A_3 = -\frac{\epsilon^3 z}{12}\phi_1\phi_2(1-2\phi_1)^2$$

$$A_4 = -\frac{\epsilon^4 z}{48}\phi_1\phi_2[1-6\phi_1\phi_2(3\phi_1^2-3\phi_1+2)]$$

$$B_1^{(lk)} = -\epsilon N(1,l)\phi_k - \frac{\epsilon}{z}N(1,l)N(1,k)$$

$$B_2^{(lk)} = \frac{\epsilon}{z}[2N(2,l) + N(3,l) + 3N(\perp,l) + [N(1,2;l) - N(1,l)N(2,l)M_l] - 4N(1,k)N(2,l)]\phi_k$$

$$B_3^{(lk)} = -\frac{2\epsilon}{z}N(1,l)[2N(1,l) + [N(1,1;l) - N(1,l)^2M_l]]\phi_l\phi_k$$

$$B_4^{(lk)} = -\frac{2\epsilon}{z}N(1,l)N(1,k)[N(1,l) + N(1,k) - 2]\phi_l\phi_k$$

$$B_5^{(lk)} = -\frac{2\epsilon}{z}N(1,l)[N(1,1;k) - [N(1,k)]^2M_k]\phi_l^2$$

$$B_6^{(lk)} = -\frac{4\epsilon}{z}[[N(1,l)]^3 - 3[N(1,l)]^2N(1,k)]\phi_l^2\phi_k$$

$$C_1^{(lk)} = -\frac{\epsilon^2}{2}N(1,l)\phi_k(1-2\phi_l)^2$$

$$C_2^{(lk)} = -\epsilon^2N(2,l)\phi_k^2$$

$$C_3^{(lk)} = -\epsilon^2[N(1,l)]^2\phi_l(1-3\phi_l)\phi_k^2$$

$$C_4^{(lk)} = -\frac{\epsilon^2}{2}[N(1,1;l) - [N(1,l)]^2M_l]\phi_k^3$$

$$C_5^{(lk)} = -3\epsilon^2N(1,l)N(1,l)\phi_l^2\phi_k^2$$

[a] The energy ϵ is expressed in units of kT. $N(\alpha,i) \equiv N_\alpha^{(i)}/M_i$; $i = 1$ and 2; $N(\alpha,\beta;i) \equiv N_{\alpha,\beta}^{(i)}/M_i$, $i = 1$ and 2.

in Table I for the athermal limit. Table III (as well as Table IV and Appendix A) use the shorthand notation of ϵ to replace ϵ/kT. The free energy of mixing is written in the formal double expansion in ϵ/kT and z^{-1} as

$$\frac{\Delta F^{mix}}{N_l kT} = \frac{\varphi_1}{M_1}\ln\varphi_1 + \frac{\varphi_2}{M_2}\ln\varphi_2 + \sum_{i=0}^{\infty} a_i(\epsilon/kT)^i \quad (3.6)$$

All terms through order z^{-2} smaller than the leading Flory–Huggins approximation are retained in the order ϵ contributions in Table III; those in ϵ^2 contain the order z^{-1} corrections to the leading extended mean-field (EMF) term; while only the leading EMF contributions of orders ϵ^3 and ϵ^4 are retained (Figure 4). The computations of the latter two terms are new and are described in Appendix A, which also elaborates on the algebraic derivation and on the use of the diagrammatic techniques for the interaction energies. The derivation of the z^{-1} correction to the ϵ^2 terms is considerably more lengthy and will be discussed elsewhere. Theories containing terms only through order a_n are called "nth order theories" below.

The special limit, where one component is a solvent covering a single lattice site per molecule, is obtained from Table III by setting $M_2 = 1$ and all $N_j^{(2)} = N_{j,i}^{(2)} = 0$. This special case is presented in Table IV for direct comparison with the Monte Carlo simulations.

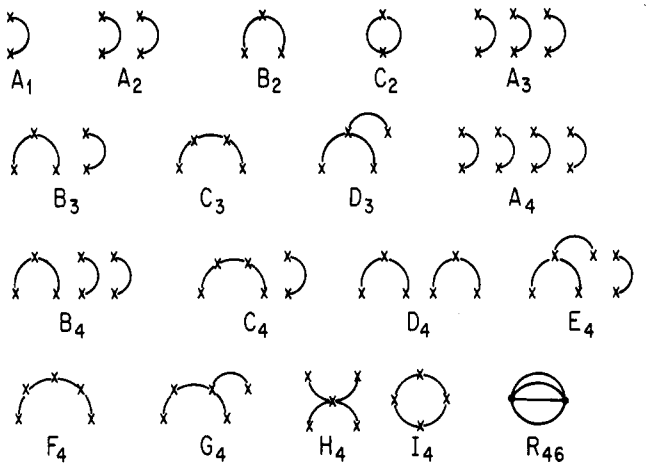

Figure 4. Extended mean-field energy diagrams (only those with interaction lines) through order ϵ^4. The subscript designates the order in the Mayer function $f \equiv \exp(\epsilon) - 1$. Also shown is a new contracted diagram R_{46} of order z^{-3} that is required here [see (A.6)].

Table IV
Free Energy of Mixing and Internal Energy of Mixing for a Polymer-Void (Solvent) System[a]

$$\frac{\Delta F^{mix}}{kTN_l\phi(1-\phi)} = \sum_{i=1}^{4} A_i + \sum_{i=1}^{4} B_i + \sum_{i=1}^{4} C_i - \frac{\Delta S_\infty^{mix}}{kN_l\phi(1-\phi)}$$

$$\frac{\Delta E^{mix}}{kTN_l\phi(1-\phi)} = \sum_{i=1}^{4} iA_i + \sum_{i=1}^{4} B_i + 2\sum_{i=1}^{4} C_i$$

$$A_1 = \frac{\epsilon z}{2}$$

$$A_2 = -\frac{\epsilon^2 z}{4}\phi(1-\phi)$$

$$A_3 = -\frac{\epsilon^3 z}{12}\phi(1-\phi)(1-2\phi)^2$$

$$A_4 = -\frac{\epsilon^4 z}{48}\phi(1-\phi)[1-6\phi(1-\phi)(3\phi^2-3\phi+2)]$$

$$B_1 = -\epsilon N(1)(1-\phi)$$

$$B_2 = \frac{\epsilon}{z}[2N(2) + N(3) + 3N(\perp) + [N(12) - N(1)N(2)M]](1-\phi)$$

$$B_3 = -\frac{2\epsilon}{z}N(1)[2N(1) + [N(11) - N(1)^2M]]\phi(1-\phi)$$

$$B_4 = -\frac{4\epsilon}{z}[N(1)]^3\phi^2(1-\phi)$$

$$C_1 = -\frac{\epsilon^2}{2}N(1)(1-\phi)(1-2\phi)^2$$

$$C_2 = -\epsilon^2N(2)(1-\phi)^2$$

$$C_3 = -\epsilon^2[N(1)]^2\phi(1-\phi)^2(1-3\phi)$$

$$C_4 = -\frac{\epsilon^2}{2}[N(11) - [N(1)]^2M](1-\phi)^3$$

[a] The energy ϵ is expressed in units of kT. $N(\alpha) \equiv N_\alpha/M$, $N(\alpha\beta) \equiv N_{\alpha,\beta}/M$.

4. Results for the Polymer–Solvent System and Comparison with Monte Carlo Simulations

Before considering comparisons between theories of the statistical thermodynamics of concentrated polymer solutions, melts, and blends, it is essential to test the accuracy of the approximations introduced in solving the model chosen to represent the physical system. Evidently, severe misinterpretations of the physics may arise from not properly separating the errors inherent in the chosen model from those made in obtaining approximate solutions

Table V
Values of the $q \neq 0$ Leading Terms of f^n and ϵ^n Diagrams ($n \leq 4$)[a]

diagram from Figure 4	symmetry factor s	d_B factor[b,c]	value of $\mathbf{q} \neq 0$ diagram[d]
A_1[e]	$\frac{1}{2}$	R_{11}^2	$N_l\phi^2 f z/2$
A_2	$\left(\frac{1}{2}\right)^2\left(\frac{1}{2!}\right)$	$2R_{21}'$	$N_l\phi^4 f^2 z/4$
B_2	$\frac{1}{2}$	$-R_{21}'$	$-N_l\phi^3 f^2 z/2$
A_3	$\left(\frac{1}{2}\right)^3\left(\frac{1}{3!}\right)$	$16R_{31}'$	$N_l\phi^6 f^3 z/3$
B_3	$\left(\frac{1}{2}\right)^2$	$-4R_{31}'$	$-N_l\phi^5 f^3 z$
C_3	$\frac{1}{2}$	R_{31}'	$N_l\phi^4 f^3 z/2$
D_3	$\frac{1}{3!}$	$2R_{31}'$	$N_l\phi^4 f^3 z/3$
A_4	$\left(\frac{1}{2}\right)^4\left(\frac{1}{4!}\right)$	$48R_{42}' + 288R_{46}'$	$3N_l\phi^8 f^4 z/8$
B_4	$\left(\frac{1}{2}\right)^3\left(\frac{1}{2!}\right)$	$-8R_{42}' - 48R_{46}'$	$-3N_l\phi^7 f^4 z/2$
C_4	$\left(\frac{1}{2}\right)^2$	$2R_{42}' + 8R_{46}'$	$N_l\phi^6 f^4 z/2$
D_4	$\left(\frac{1}{2}\right)^2\left(\frac{1}{2!}\right)$	$2R_{42}' + 10R_{46}'$	$N_l\phi^6 f^4 z/2$
E_4	$\left(\frac{1}{2}\right)\left(\frac{1}{3!}\right)$	$12R_{46}'$	$N_l\phi^6 f^4 z$
F_4	$\frac{1}{2}$	$-R_{42}' - 2R_{46}'$	$N_l\phi^5 f^4 z/2$
G_4	$\frac{1}{2!}$	$-2R_{46}'$	$-N_l\phi^5 f^4 z$
H_4	$\frac{1}{4!}$	$-6R_{46}'$	$-N_l\phi^5 f^4 z/4$
I_4	$\left(\frac{1}{4}\right)\left(\frac{1}{2}\right)$	$R_{42}' + R_{46}'$	$-N_l\phi^4 f^4 z/4$
ϵ diagram			$N_l\phi^2\epsilon z/2$
sum of all ϵ^2 diagrams			$N_l\phi^2(1-\phi)^2\epsilon^2 z/4$
sum of all ϵ^3 diagrams			$N_l\phi^2(1-\phi)^2(1-2\phi)^2\epsilon^3 z/12$
sum of all ϵ^4 diagrams			$N_l\phi^2(1-\phi)^2[1-6\phi(1-\phi)$ $(3\phi^2-3\phi+2)]\epsilon^4 z/48$

[a] $f = \exp(\epsilon) - 1$. $\phi = Mn_p/N_l$; M is the total number of lattice sites that a polymer chain occupies. [b] $D_B \equiv d_B\alpha$; $\alpha = [N_l(N_l-1)\cdots(N_l-n_v-1)]^{-1}$ and D_B represents the value of an entropy diagram with B bonds [see (2.13) and ref 15]. [c] Only z^{-n+1} terms of the contracted diagram R_{nm} are necessary and therefore are retained. [d] Only $N_l z$ terms are retained. Higher order terms in N_l and in z are cancelled when forming cumulants and when summing together diagrams with $\mathbf{q} = 0$ contributions. [e] Only the $\mathbf{q} = 0$ term contributes to diagram A_1.

to that model. Here we test the internal consistency of several approximate solutions to the standard lattice model by comparing lattice theory predictions with Monte Carlo simulations *for the identical system*.[21] These comparisons involve no adjustable parameters, so the sole criterion for the accuracy of the approaches is the degree to which they reproduce the Monte Carlo data (within the statistical uncertainty of the method). Details of the Monte Carlo simulation methods as well as tests of its accuracy are exhaustively presented in ref 5 and references cited therein. Thus, the description of these methods is not repeated here.

Madden et al.[5] have compared the Pesci–Freed lattice cluster theory calculations for linear polymers and single-bead solvent molecules with the results of computer simulation for the identical lattice model, the Flory lattice theory (called Flory–Huggins theory in the literature), and several versions of the Guggenheim lattice theory[12] as follows: The Guggenheim random-mixing theory (GRM) is first order in ϵ and therefore does not include changes in chain configurations induced by the van der Waals interactions. The Guggenheim quasi-chemical (GQC) approximation introduces some of these configuration changes and is essentially a second-order theory.[5] Madden et al. show that the athermal free energy of mixing for the cluster theory is nearly identical with that of the athermal limit of the Guggenheim theory but distinctly different from that of traditional Flory–Huggins theory. Though Madden et al. present no computer simulations of this quantity, earlier simulation studies by Dickman and Hall[8] establish that the excess chemical potential of a single-

bead solvent (the "pressure" in a lattice fluid model) is much better represented by the Huggins–Miller[22]–Guggenheim theory and by Freed's lattice cluster theory (to order z^{-2}), with the edge going to the cluster theory as the length of the chains is increased. The ability of Dickman and Hall to distinguish between these theories illustrates the important point that many thermodynamic properties depend on derivatives of the free energy of mixing and are thus quite sensitive to very subtle differences in that quantity.

A. Energy of Mixing. Madden et al. also present a direct determination of the first-order correction e_1 in the internal energy of mixing

$$\frac{\Delta E^{\text{mix}}}{N_l kT} = \sum_{i=1}^{\infty} e_i(\epsilon/kT)^i \tag{4.1}$$

for a linear polymer–single-bead solvent system as a function of polymer volume fraction. These e_i values are related to the corresponding expansion of the free energy of mixing of (3.6) by $e_i = ia_i$. The Guggenheim prediction for $e_1 = a_1$ agrees well with the simulation data and nearly as well with the Pesci–Freed prediction (calculated in the $M_1 = \infty$ limit). The standard Flory–Huggins prediction for e_1 is found to be substantially poorer. Despite the remarkable similarity between the Guggenheim theory and Pesci–Freed calculations for the zeroth (a_0) and first-order (a_1) terms in the expansion of the free energy of mixing, the coexistence curves calculated from the corresponding first-order theories agreed well only at high-volume fractions. The Pesci–Freed coexistence curves are found to be in very poor agreement with simulation (worse than Flory–Huggins theory) near the critical point. This had led Madden et al.[5] to conclude that it is crucial to include the full molecular weight dependence of all diagrams to at least first order in the expansion in ϵ, and this has been done in the new expressions presented in the tables.

Figure 5 shows the Monte Carlo data for the internal energy of mixing for the polymer–solvent system at $kT/\epsilon = \infty$ and at $kT/\epsilon = 3$. The infinite temperature limit for the internal energy of mixing per lattice site is just $e_1 = a_1$. The uncertainty in the simulation data is believed to be smaller than the range spanned by the symbols. The first-order prediction from the terms of order ϵ in Table IV and from the first-order Guggenheim theory (GRM theory) are both in impressive agreement with the $kT/\epsilon = \infty$ simulations and are substantially better than the energetic contribution to the Flory–Huggins theory. Also shown are the simulation data for $kT/\epsilon = 3.00$. No simulation points are presented for polymer volume fraction between 0.03 and 0.4 because the simulation sample undergoes phase separation at this temperature. The internal energy predicted by the Guggenehim quasi-chemical (GQC) approximation and by the cluster theory (LCT) to second order are also displayed in Figure 5. The terms of order ϵ^3 and ϵ^4 in the tables are found to provide negligible contributions. (Polymer connectivity and monomer geometry are included in the equations of the tables only through second order in ϵ.) The cluster theory is seen to provide a better estimate of the contribution of the higher order terms in the expansion of the internal energy than all previous theories.

The energy of mixing for linear polymers $M_1 = 100$ with linear solvents $M_2 = 5$ is presented in Figure 6 as a function of temperature to illustrate the small, but nontrivial, effect that is predicted by the lattice cluster theory and has been ignored in Flory–Huggins and other theories. The general trend of temperature dependence in Figure 6 is in accord with observations made for polymer blends.

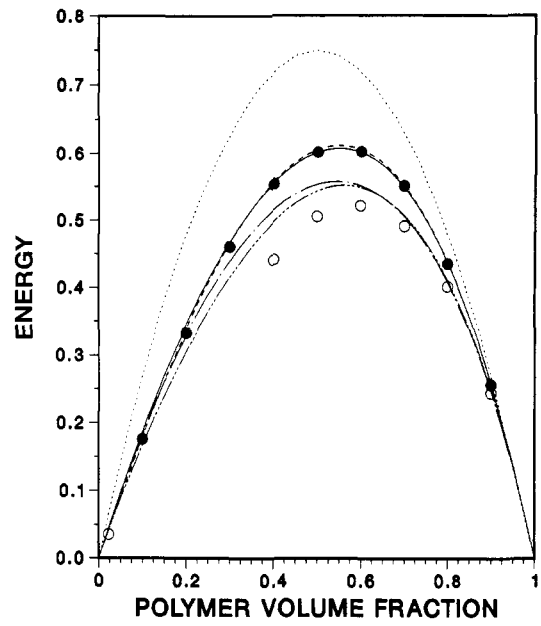

Figure 5. Dimensionless energy of mixing $\Delta E^{\text{mix}}/(N_l\epsilon)$ for solutions of linear polymers ($M_1 = 100$) in single-bead solvents ($M_2 = 1$) as a function of polymer volume fraction. Solid symbols are Monte Carlo results for $T^* = \infty$. Theoretical curves: (···) Flory–Huggins, (—) GRM; (- - -) LCT1 (first order in ϵ). Open symbols are Monte Carlo results for $T^* \equiv kT/\epsilon = 3$. Theoretical curves at $T^* = 3$: (– · –) GQC; (– · · · –) LCT2 (through second order in ϵ). (Second- and fourth-order versions of the lattice cluster theory are not distinguishable.)

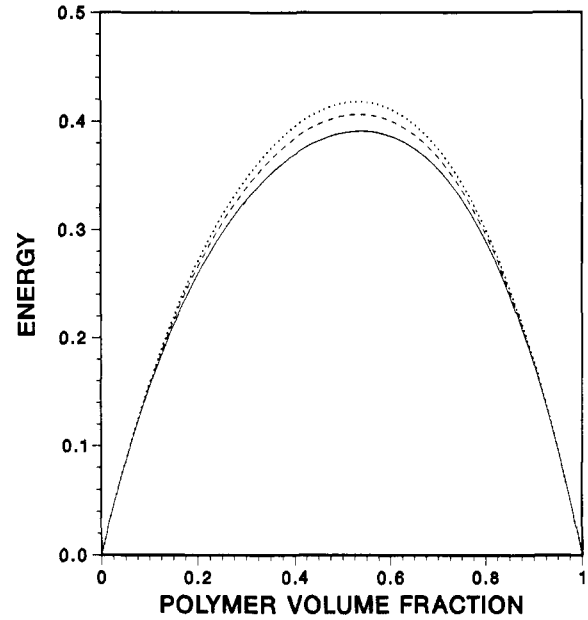

Figure 6. Lattice cluster theory predictions for the dimensionless energy of mixing $\Delta E^{\text{mix}}/(N_l\epsilon)$ for solution of linear polymers ($M_1 = 100$) in linear solvents ($M_2 = 5$) as a function of temperature: (—) $T^* = 3.0$; (- - -) $T^* = 3.5$; (···) $T^* = 4.0$.

Madden et al. also estimate the magnitude of the second-order term e_2 by fitting simulation data near the athermal limit to straight lines at several volume fractions and by finite difference estimates at other concentrations. They determine that the Guggenheim quasi-chemical approximation is essentially second order in this application (higher order terms, though formally present, prove to be negligible) and that the Pesci–Freed second-order term is much too large and of the wrong sign. The second-order internal energy of mixing ($e_2 = 2a_2$) predicted by the equations of Table IV is compared in Figure 7 with the

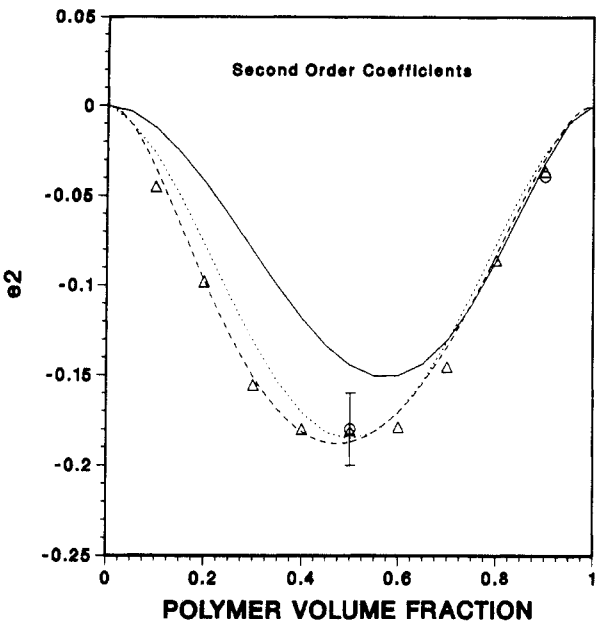

Figure 7. Second-order term e_2 of (4.2) as a function of polymer volume fraction. Circles are Monte Carlo estimates based on fits to plots of $\Delta E^{min}/N_l$ vs ϵ at high temperatures. Triangles are Monte Carlo estimates obtained from single finite differences at high temperatures. (For more details see ref 5.) Theoretical curves: (—) GQC; (···) EMF; (- - -) LCT.

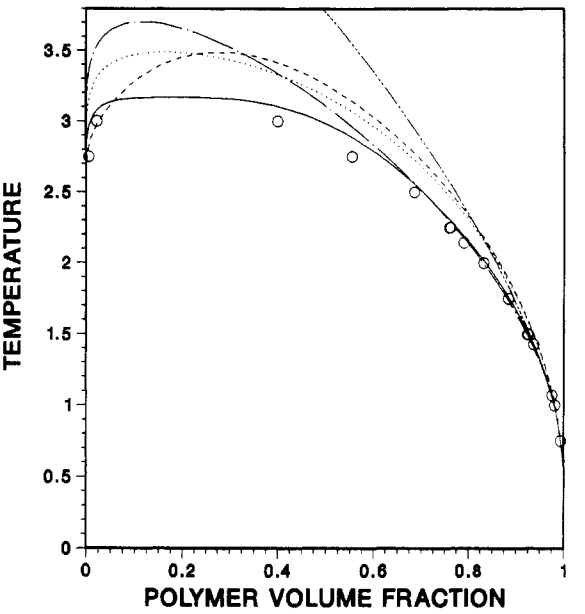

Figure 8. Coexistence curve for a mixture of linear polymer (M_1 = 100) and single-bead solvents (M_2 = 1). Circles are Monte Carlo results. Theoretical curves: (— · · · —) Flory–Huggins; (···) GRM; (— · —) GQC; (- - -) LCT1 (first order in ϵ); (—) LCT2 (through second order in ϵ). The ordinate is the reduced temperature $T^* = kT/\epsilon$ as in all the following figures, except Figure 13.

simulation estimates and the second-order term from the Guggenheim theory. Also shown is e_2 from the extended mean-field (EMF) theory, which Madden et al. concluded was the best available estimate for this term. The EMF approximation is obtained from the cluster theory by retaining only interaction lines and no correlating bonds in the expansions of (3.3) and hence discards entirely the chain character of the polymer. The present calculation, which includes many diagrams neglected by Pesci and Freed, clearly gives e_2 in best agreement with the estimates made by the simulations.

B. Coexistence Curves. One of the most sensitive tests of any theory of the free energy of mixing is the determination of coexistence curves. In order to predict these curves, the theory under consideration must accurately describe the chemical potentials of the two species in both phases or must make proportionate errors in their calculations. Traditional lattice theories assume that an intramolecular contribution can be factored out of the partition function and that this contribution is independent of composition.[10,12] While this assumption seems reasonable at high polymer volume fractions where there is significant screening, it is patently untrue in dilute and semidilute solutions. The composition dependence of the intramolecular configurational factor is manifest in a variety of structural properties, the crudest of which is the radius of gyration of a single chain in the system. Madden et al.[5] show that the radii of gyration of linear polymers in a single-bead solvent exhibit measurable variation with composition, even for polymer volume fractions above 0.5. The traditional Flory, Huggins, and Guggenheim theories make no allowance for the compositional dependence of the intramolecular structure, while the lattice cluster theory cannot but include such effects because it employs an *exact* formal expansion in ϵ and z^{-1}. However, Madden et al. note that the expansions employed by Freed and co-workers are not faithful to the known results in certain scaling regimes, such as the semidilute limit (where the osmotic pressure varies as roughly the $^9/_4$ power of the volume fraction in the scaling limit[23]). This failing is shared by the traditional theories, which are all of a mean-field variety and therefore cannot describe the long-range correlations inherent in the dilute and semidilute limits. However, following the arguments of Flory[9] and de Gennes,[23] the dominant correlations in concentrated polymer solutions, melts, and blends are believed to be short range in nature and therefore amenable to mean-field treatments such as the present cluster theory.

Figure 8 presents Monte Carlo data and several lattice theory predictions for the coexistence curves of linear polymers in single-bead solvents. The calculations and simulations assume that ϵ of (2.1) is positive so that the polymer–solvent system has an upper critical solution temperature. A negative ϵ produces a lower critical solution temperature. Theories containing a_i for $i \geq 2$ in (3.6) lead to some asymmetry between these two cases, but the general behavior is quite similar. The Flory–Huggins result in Figure 8 has an off-scale critical temperature of 4.96 and is clearly the worst of the lot. The first-order lattice cluster theory (LCT1 includes only a_0 and a_1) and the first-order Guggenheim theory (GRM) coexistence curves are nearly identical at high polymer volume fractions but are slightly poorer than the Flory–Huggins theory at these higher volume fractions because the latter benefits from a considerable cancellation of errors at such concentrations. Both GRM and LCT1 theories give a similar critical temperature, but the first-order cluster theory predicts a critical volume fraction that is higher than any of the other theories and seems inconsistent with the available simulation data.

Also shown in Figure 8 are three coexistence curves that include higher order temperature dependences beyond a_1. The Guggenheim quasi-chemical approximation provides excellent predictions for polymer volume fractions higher than 0.7, but it deteriorates somewhat at lower volume fractions and yields a rather high critical temperature. The figure clearly demonstrates that inclusion of the proper, structure-dependent, second-order contribution produces a coexistence curve having the best agreement with the simulation data.[24] Addition of the EMF third- and fourth-order terms from Table IV produces a coexistence curve (not shown) that is only very slightly different from the

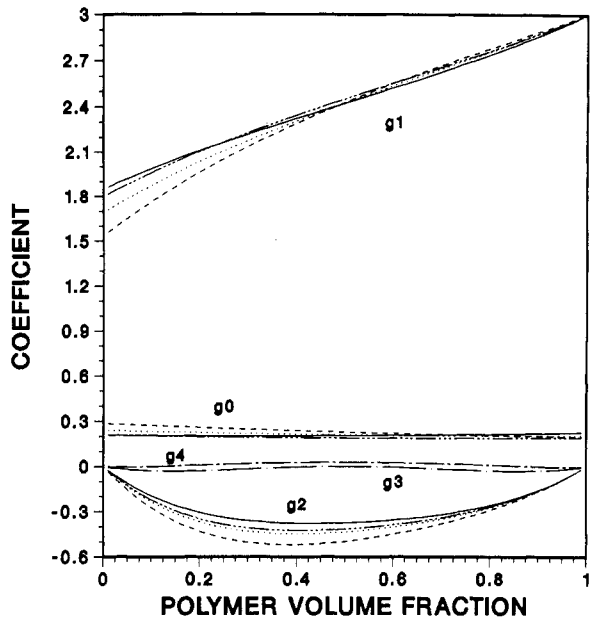

Figure 9. LCT contributions to an effective parameter χ [see (4.2)] as a function of polymer volume fraction for different chain morphologies (see Figure 1). The polymer is of molecular weight $M_1 = 100$ (or 101 for type c chains). Each solvent is a single bead ($M_2 = 1$), while the polymer structures are as follows: (—) polymer type a; (- - -) polymer type b; (· · ·) polymer type c; (– · · · –) polymer type d.

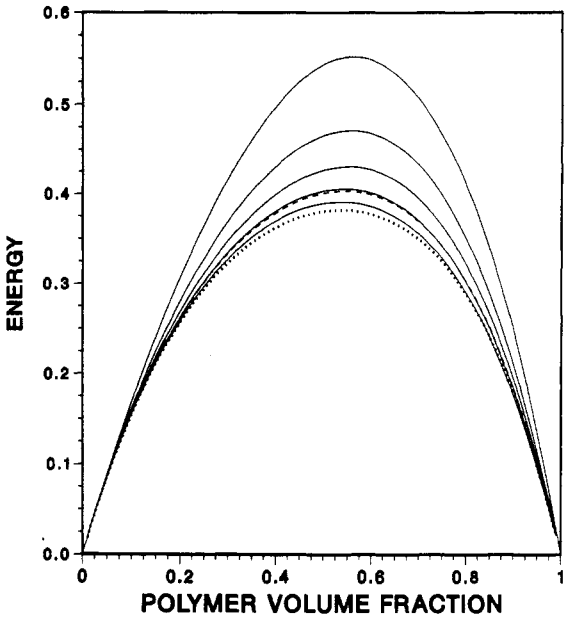

Figure 10. Lattice cluster theory prediction of the dimensionless energy of mixing $\Delta E^{mix}/(N_l\epsilon)$ as a function of volume fraction and of polymer and solvent structure. The polymer molecular weight is 100. Solid curves: solvent type a, molecular weights 1–5 (top to bottom). Dashed curve: solvent type b, molecular weight 4. Dotted curve: solvent type c, molecular weight 5. All curves are for $kT/\epsilon = 3.0$.

curve presented for the second-order cluster theory.

We also have attempted to continue the $1/z$ and ϵ expansions of the cluster theory by constructing [1,0] Padé approximants from the last two terms in the $(1/z)$ expansion of the individual terms in the ϵ expansion and then constructing another [1,0] Padé from the first- and second-order terms of the ϵ expansion of the free energy of mixing. For polymer volume fractions above 0.55, the resulting coexistence curve is indistinguishable from that shown for the second-order cluster theory. It becomes somewhat poorer at lower volume fractions and yields a critical temperature of 3.24. For clarity, this curve is not displayed in the figure. The insensitivity of the computed coexistence curves to formation of Padé approximants at higher volume fractions and the diminution of available higher order contributions in both expansions augur well for the practical convergence of these expansions in the cluster theory.

C. Influence of Monomer and Solvent Structure. One of the principal strengths of the cluster theory is its ability to include the effects of different chain and solvent morphologies on the free energy of mixing. In this report, we consider the polymers and solvents based on the structures shown in Figure 1. (A wide range of other structures will be discussed elsewhere in applications to polymer blends.) In Figure 1 the chain ends are capped by a single bead. The appropriate coefficients $N(i;l)$, etc., may be found in the papers by Nemirovsky et al.[15] and Pesci and Freed.[25] In order to display the thermodynamic differences more clearly, we write the free energy of mixing as

$$\frac{\Delta F^{mix}}{N_l kT} = \frac{\varphi_1}{M_1}\ln\varphi_1 + \frac{\varphi_2}{M_2}\ln\varphi_2 + \varphi_1\varphi_2\sum_{n=0}^{\infty} g_n(\epsilon/kT)^n \qquad (4.2)$$

where the g_n are the coefficients of a reciprocal temperature expansion of an effective χ parameter (not to be confused with that obtained from extrapolations to zero angle of neutron scattering data[26]). Figure 9 presents the g_n for chains of length 100 or 101 mixed with a single-bead solvent. The calculations for g_0 show that the athermal correction to the Flory–Huggins entropy is nearly identical for all four chain architectures of Figure 1 at high polymer volume fractions, but the differences become increasingly significant in the dilute solutions limit. These differences would be difficult to discern in a comparison of the individual a_n because those quantities vanish in either pure substance limit.

The first-order correction, g_1, behaves in a similar fashion, with even larger differences appearing in the dilute limit. In the pure polymer limit, g_1 approaches the Flory–Huggins result of $z/2$ for all architectures. [Note that the thermal version of the cluster theory assigns an interaction energy to every pair of adjacent beads, whether or not they are covalently bonded. This causes a shift in the zero of energy for the pure components, which is eliminated in the subtractions required to construct the free energy of mixing.] Both g_0 and g_1 are positive for all compositions. By contrast, the second-order correction, g_2, is everywhere negative and vanishes in the pure-component limits. However, for the dilute polymer limit, the slope of g_2 is distinctly different for the architectures a, b, and c. This is significant because the compositional derivatives of the g_n also contribute to the chemical potentials. The most substantial differences in g_2 are found at intermediate volume fractions and especially near the critical volume fractions shown in Figure 8. Thus, the form of g_2 markedly influences the calculated coexistence curve. The EMF approximations g_3 and g_4 derived from the equations of Table IV are also displayed in Figure 9. They are independent of chain architecture and are quite small at all compositions.

Solvent structure and size also influence the noncombinatorial entropy of mixing and the energy of mixing of the polymer–solvent system. Figure 10 illustrates this feature of the theory in Table III by presenting ΔE^{mix} for a solution of a linear polymer with $M_1 = 100$ in a range of linear solvents with $M_2 = 1, \ldots, 5$ and with a type b solvent of $M_2 = 4$. There is a rather strong dependence on solvent size, with the energy of mixing decreasing as

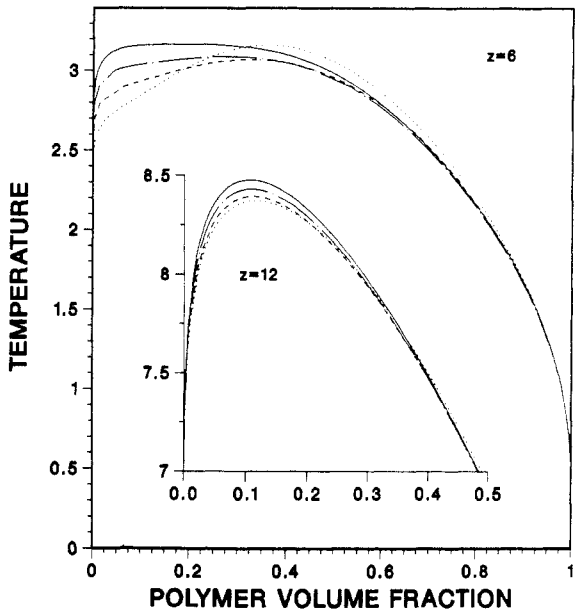

Figure 11. Second-order LCT coexistence curves for polymers of various morphologies with single-bead solvents. The polymer molecular weight is 100 (101 for type c chains). The curves are labeled as follows: (—) polymer type a; (- - -) polymer type b; (· · ·) polymer type c; (– · –) polymer type d. The main figure is for three dimensions ($z = 6$). The inset depicts the critical region in six dimensions ($z = 12$).

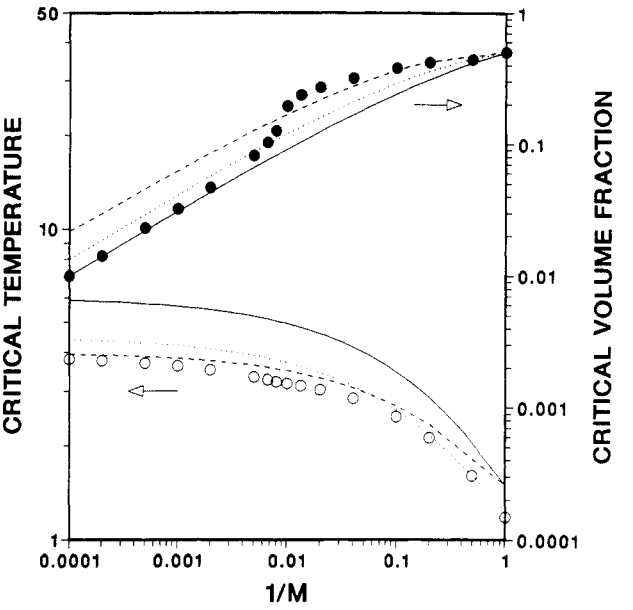

Figure 12. Critical constants for a linear polymer–single-bead solvent system as a function of reciprocal polymer molecular weight. Upper curves (right axis) are critical polymer volume fractions. Lower curves (left axis) are critical reduced temperatures. Symbols designate the second-order LCT, and the other curve are as follows: (—) Flory–Huggins; (- - -) GRM; (· · ·) GQC. Axes are logarithmic.

the solvent size increases. This structure dependence does not appear in the Flory–Huggins theory because the latter is independent of molecular structure. While the noncombinatorial entropy of mixing for the two geometrical isomer solvent molecules for $M_2 = 4$ differ as expected, there is even a slight, but perceptable, difference in the energy of mixing in Figure 10, and the difference grows for the geometrical isomers with $M = 5$.

Figure 11 shows the coexistence curves for chains with $M_1 = 100$ or 101 for polymer architectures of Figure 1 and a single-bead solvent. The cluster theory (to order ϵ^{-2}) predicts substantially different phase envelopes. All agree well at the highest volume fractions. The linear polymer (Figure 1a) and the simply branched polymer (Figure 1b) coexistence curves differ only near the critical temperature. The similarity of the curves at high volume fractions indicates that the three chain architectures also have similar low-pressure melt equations of state when the solvent molecules are regarded as vacancies and the theory is given a lattice-fluid interpretation. The most significant differences among the coexistence curves are the predicted critical volume fractions and their shapes near the critical point. There are reasons to suspect that the present cluster theory computations may not be sufficiently adequate at low values of z for polymers with the crowded architecture of Figure 1c. The structures a–c are distinguished by the presence of beads with increasingly high valency. The cluster expansion of the free energy contains coefficients associated with the number of ways in which multiple covalent bonds may simultaneously emanate from a single bead. The linear polymer has at most two such bonds, and their presence is reflected in the coefficients $N(i,j;l)$. Trivalent structures, such as that of Figure 1b, generate a new coefficient $N(\perp;l)$; tetravalent structures of Figure 1c, provide still another, $N(+;l)$.

All such coefficients appear in the expansion of the overall free energy within terms multiplied by a linear power of the volume fractions, but such contributions do not all persist in the free energy of mixing to the order computed in the tables presented here. The coefficients, however, enter again at some higher power in the expansions in $1/z$. Examination of the tables presented here shows that the tetravalent parameter $N(+;l)$ does not contribute to the expressions employed in calculating the coexistence curves. It seems at least plausible that this important measure for the effects of the organization of the tetravalent monomer may have substantial impact on the predicted coexistence curve. Further evidence that the expressions presented here are not entirely adequate for structures of Figure 1c arises when the chain lengths are varied. The critical composition for polymers with that architecture does not approach zero as the chain length is increased but instead seems to approach an unphysical limiting value of about 0.35. We attribute the error for this structure to a premature truncation of the $1/z$ expansion, which eliminates the important $N(+;l)$ contributions to the chemical potentials. At higher values of z (higher dimensionalities) the coexistence curves are much less sensitive to the chain architectures. This is illustrated for $z = 12$ ($d = 6$) in the inset in Figure 11. Whether this holds true for close-packed lattices in three dimensions remains to be seen. However, in either situation the expansion in z^{-1} is expected to be more rapidly convergent for these lattices than those in the $z = 6$ ($d = 3$) case. The additional conformational freedom in the neighborhood of a tetracovalent bead on high z lattices may mean that the omitted terms in $N(+;l)$ are truly negligible.

For the second-order cluster theory used in most of the calculations reported here, critical compositions for the a and b architectures properly approach zero concentration of polymer as the chain length is increased. Curiously, when the cluster theory is truncated at first order in ϵ, the anomalies described above for the c architecture are present for all three chain types. Presumably, there is some cancellation of errors between the truncated $1/z$ expansions of a_0, a_1, and a_2, which eliminates the problem at second order in ϵ. Figure 12 shows a log–log plot of φ_c and T_c vs $1/M_1$ for several approximations to the lattice model. Note that the first-order Guggenheim theory (GRM) does not

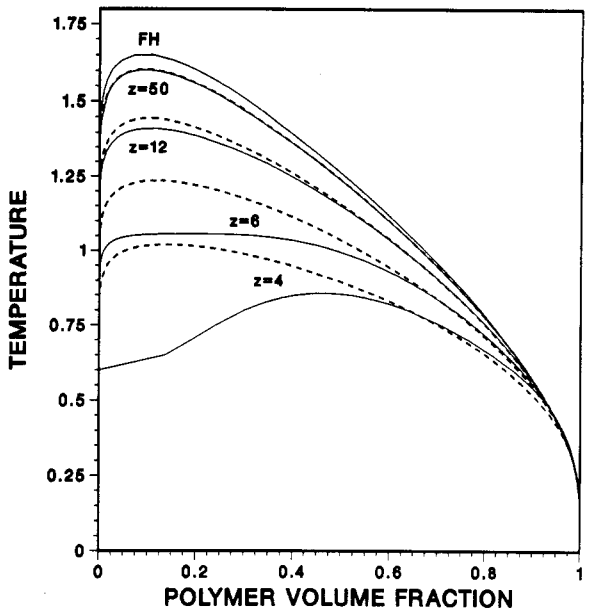

Figure 13. Coexistence curves for a linear polymer (M_1 = 100)–single-bead solvent system as functions of lattice coordination number z. The Flory–Huggins (FH) theory corresponds to $z = \infty$. Dashed curves: GQC. Solid curves: second-order LCT. The LCT theory is for a simple hypercubic lattice with dimensionality $z/2$. The reduced temperature is in units of the reciprocal Flory χ parameter (for this figure *only*).

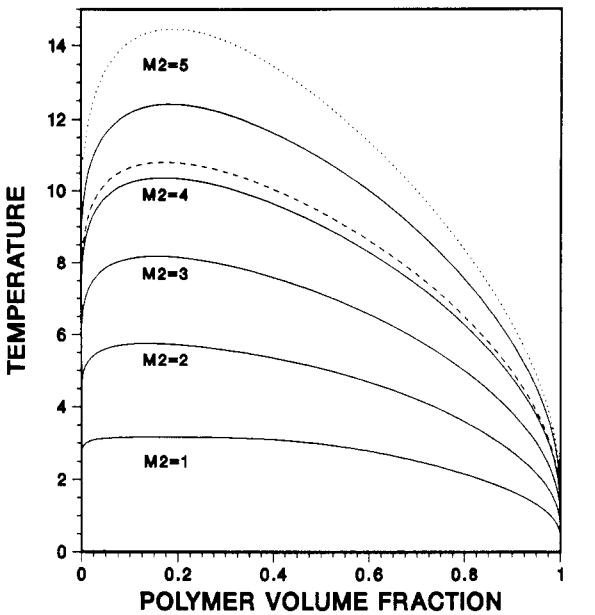

Figure 14. LCT coexistence curves for linear polymer (M_1 = 100)–solvent systems. Molecular weights of the solvent are in the range 1–5 (top to bottom). Solid curve: linear solvent type a. Dashed curve: solvent type b ($M_2 = 4$). Dotted curve: solvent type c ($M_2 = 5$). See Figure 1 for the key to solvent morphologies.

suffer from the difficulties described for the first-order cluster theory because it completely ignores intramolecular conformational changes in dilute solution. The cluster theory calculations exhibit kinks in the plots of the critical constants (which are nearly imperceptible in linear plots). The origins of these kinks are unclear, but they are associated only with the very tops of the coexistence curves, which are unremarkable in all other respects.

Figure 13 shows the coexistence curves for linear polymers with single-bead solvent molecules at several values of the coordination number, z. In order to eliminate the dramatic effect that variation of the coordination number has on the critical temperature, the temperature is reported in Figure 13 as the reciprocal of the Flory–Huggins χ parameter and is smaller than the reduced temperature used elsewhere by a factor of $2/z$. The cluster theory computations involve a summation over the first Brillouin zone of the reciprocal lattice and thus discriminate among various lattice geometries with the same coordination number. The equations shown in the tables are specifically for simple hypercubic lattices. Hence, the cluster theory predictions for a particular value of z are therefore to be associated with a hypercubic lattice in a $d = z/2$ dimensional space. The Guggenheim theories do not consider any secondary lattice structure and therefore make no distinction between, say, a simple cubic lattice in six dimensions and an fcc lattice in three dimensions or between a two-dimensional square lattice and a three-dimensional diamond lattice. In the limit of infinite coordination number, both theories become equivalent to the Flory–Huggins theory, which is exact in that limit. (Thus, the extended mean-field theory at finite z is not equivalent to taking the $z = \infty$ limit. The latter limit supresses the contributions of the higher order terms in the ϵ expansion because of the necessary rescaling of the temperature.)

At $z = 50$ the Guggenheim theory and the cluster theory give coexistence curves that are nearly identical and that are discernibly different from the limiting Flory–Huggins curve. At $z = 12$, the two theories yield slightly different curves, while for $z = 6$ significant differences (previously reported in Figure 8) are observed. The cluster theory for $z = 4$ gives a very oddly shaped coexistence curve. However, polymer–polymer correlations are thought to be very different in two dimensions because intimate intermixing and melt screening are no longer possible. It is unlikely that the cluster theory is giving the correct result in this anomalous limit, but the origins of the peculiar shape of the coexistence curve may rest in the strange physics of two-dimensional chains. (Recently, Binder[27] has found that the mean-field approximation is invalid for two-dimensional polymer mixtures.) The Guggenheim theory makes no recognition of the dimensionality of the system, and the $z = 4$ predictions of that theory are probably appropriate only for a diamond lattice in three dimensions.

Figure 14 presents the coexistence curve of a linear polymer (M_1 = 100) with linear type a solvents of molecular weights 1–5. Also shown is the coexistence curve for linear polymers with type b solvent molecules (cf. Figure 1) of molecular weight 4 and type c solvent molecules of molecular weight 5. The structure of the solvent appears to have a significant impact on the shapes of the coexistence curves. These effects are explored more fully in Figure 15, where various combinations of solvent and polymer architecture are considered. Again, substantial differences are observed in the coexistence curves. In view of the comments made earlier, the coexistence curves produced by type c architectures must be regarded as somewhat suspect. However, the anomalies in the molecular weight dependence of the critical volume fraction of type c chains disappear whenever the solvent is of molecular weight 3 or larger. It may be that the terms involving $N(+;l)$ are somehow screened out when the solvent is larger, but we know of no way to test this speculation with the equations at hand.

5. Discussion

The algebraic derivation of the lattice cluster theory is presented for the systematic computation of corrections to the Flory–Huggins approximation for the thermodynamic properties of polymer fluids. Calculations for the

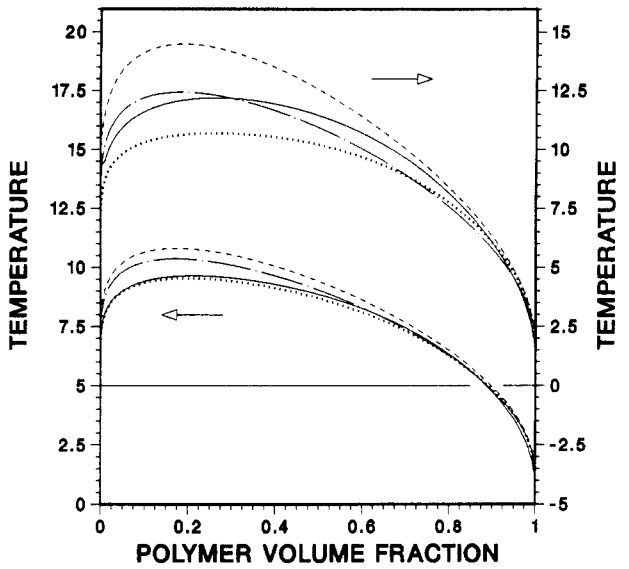

Figure 15. LCT coexistence curves for polymer–solvent systems of various morphologies for both components (cf. Figure 1). In the upper curves (right axis) the polymer molecular weight is 101 and the solvent molecular weight is 5. The curves correspond to the following (– · –) [a,a] (polymer type a, solvent type a); (- - -) [a,c]; (—) [c,a]; (· · ·) [c,c]. In the lower curves (left axis) the polymer molecular weight is 100 and the solvent molecular weight is 4. The curves correspond to the following: (– · –) [a,a]; (- - -) [a,b]; (—) [b,a]; (· · ·) [b,b].

free energies of mixing for incompressible polymer–solvent and polymer–polymer mixtures are provided as well as those for compressible polymer melts. The calculations for a hypercubic lattice involve a systematic expansion in powers of z^{-1} and of ϵ/kT for the noncombinatorial free energy of mixing, where z is the number of neighbors to a lattice site and ϵ/kT is the dimensionless effective van der Waals attractive energy of (2.1). This lattice cluster theory differs in several respects from previous theories of polymeric fluids that are not amenable to systematic improvement. First of all, we are able to treat the detailed molecular structure of monomers and of solvent molecules by permitting them to extend over several lattice sites. In addition, there is no assumption, as made in prior theories, that the intramolecular partition function is unchanged as a result of mixing. In fact, we are unable to introduce such an approximation in our systematic approach. Lastly, the theory incorporates changes in average polymer conformations that are induced by the van der Waals interactions, as is evident from the explicit temperature dependence of the entropy of mixing.

The lattice cluster theory is compared with the Monte Carlo simulations of ref 5 for the polymer–solvent system, and this provides a stringent test of the former because no adjustable parameters are involved in the comparison. Tests are applied individually for the terms in the expansion for the energies of mixing in powers of ϵ/kT as well as for the coexistence curve. The agreement for the leading first-order term is excellent, while that for the second-order $(\epsilon/kT)^2$ contributions is very good. The leading third- and fourth-order terms are found to be negligible for the temperatures considered, but there is some discrepancy between the lattice cluster theory and the simulation energy of mixing at a reduced temperature of $kT/\epsilon = 3$ that we are at a loss to explain unless, for instance the next third-order contribution is significant. Unfortunately, the higher corrections involve very lengthy computations that are probably beyond the capabilities of analytical treatments and that will therefore have to await the development of computer-assisted methods. Nevertheless, the lattice cluster theory and simulations of the coexistence curve are in good agreement, provided the full expressions from Table IV are employed. These expressions include a compositionally dependent internal energy, modifications of average polymer configurations due to interactions, and alterations of the intramolecular partition function with mixing, features that are wholly or partially absent from prior treatments. The lattice cluster theory now unambiguously provides the best theoretical description of the lattice model for the linear polymer–monomeric solvent system, but very low z or very crowded polymer and/or solvent structures may require additional terms in the z^{-1} expansion.

The good agreement with Monte Carlo simulations attests to the accuracy of the lattice cluster theory, and therefore the latter theory is used here to investigate the role of monomer and solvent structure on the energies of mixing and coexistence curves of the polymer–solvent system. Strong structural dependences are exhibited, and the energy of mixing even shows a small, but discernible, difference between solvent molecules that are geometrical isomers.

Our agreement with Monte Carlo calculations raises interest in comparisons with experimental data for concentrated polymer solutions, but at this juncture caution is necessary because of the approximate nature of the lattice model. First of all, our calculations treat each linkage as completely flexible, whereas the actual polymers and solvent molecules have bonds that are semiflexible. The lattice cluster theory can be applied to semiflexible bonds,[28] but the computational methods have yet to be developed enabling us to consider a comparable expansion in z^{-1} and ϵ/kT for this case. In addition, it is recognized that, even upon introduction of structured monomers, each lattice site is in fact occupied by a group of atoms whose interaction energies depend intimately on the chemical composition. Thus, for example, the backbone and side-group units on type b chains have different interaction energies with each other and with solvent molecules, an unfortunate aspect of nature that may be treated within the lattice cluster theory but only at the expense of introducing a whole family of interaction energies. These and other deficiencies of the lattice model, noted below, emphasize that our calculations are to be used as a qualitative indication of the role of molecular structure, configuration-dependent interactions, and interaction-dependent chain conformations, rather than as a quantitative description of real polymeric fluids.

Apart from the compressible melts (the polymer-void system), our treatment of the polymer–solvent and polymer–polymer mixtures assumes these polymer fluids to be incompressible. However, these systems are liquids and therefore must be roughly as compressible as the corresponding monomeric fluid mixtures. Thus, they must have free volumes (modeled as voids in the lattice theory) of the order of 10–20%, and the generalization of the lattice cluster theory to compressible polymer–solvent and polymer–polymer systems is currently in progress. Unfortunately, this more realistic case leads to much lengthier expressions than those in the tables, and there is a separate dependence on all three interaction energies.

Aside from some known deficiencies in modeling free volume through the use of a lattice model with voids,[29] there are other modifications of the lattice model thay may be introduced to improve its representation of reality. First of all, the attractive interactions ϵ_{ij} may be computed using Lennard-Jones[30] or van der Waals[31] interactions that are evaluated at average interunit separations. The lattice

constant may even be allowed to be temperature dependent to account for some deficiencies in describing thermal expansion solely by introducing voids.

It is useful to compare the lattice cluster approach to complementary continuum type models of polymer melts and blends. Recently, Schweizer and Curro[32] have applied approximate, nonperturbative integral equation methods to polymeric fluids. These methods are of interest in ultimately providing a fully realistic description of polymer fluids, but they have inherent limitations as does the lattice theory. Schweizer and Curro employ models of monomers with hard-core repulsions and Lennard-Jones attractions, models that are extremely crude descriptions of real monomer structures and orientation-dependent interactions. It is quite unlikely that these hard-sphere Lennard-Jones continuum models could provide true first principle predictions for actual polymers, such as polystyrene, poly(ethylene oxide), etc., because of the extreme sensitivity of polymer properties to the effective interaction parameter ϵ of (2.1). It is also unlikely that more complicated interaction potentials, such as those obtained from molecular mechanics methods, are accurate enough to evaluate the effective ϵ and hence the phase-separation temperatures with any degree of confidence. Thus, both the continuum and lattice approaches must proceed as models whose full utility and potential remains to be attained. The lattice models have an important position in polymer theory, independent of their ultimate faithfulness to real polymer, so advances with these methods are of inherent interest themselves. Likewise, the continuum methods of Curro and Schweizer represent a natural outgrowth of simple liquid theories to polymers that are also of interest in themselves. Both the lattice and continuum theories have differing advantages and disadvantages that make them somewhat complementary.

The RISM methods employed by Curro and Schweizer involve uncontrolled approximations whose validity for polymers has recently been checked by comparison with Monte Carlo compuations,[33] and the agreement is good provided that an accurate single-chain intramolecular structure factor, e.g., one from Monte Carlo simulations, is introduced into the RISM method. This sensitivity of the RISM method to the intramolecular correlation function has led Curro and Schweizer to focus on the importance of the correlation hole in polymer melts and blends in apparent contradiction with the common belief, following Flory[9] and de Gennes,[23] that only short-range correlations are important in these systems. However, the total structure factors presented in ref 33 exhibit structure only out to about the third nearest neighbors, very much as in a fluid of small molecules. Similarly, accurate results emerge from the lattice cluster theory only at order z^{-2} where diagrams including up to four bonds are included. These diagrams introduce both intra- and intermolecular short-range correlations out to distances of third nearest neighbors, and, therefore, the accuracy requirements on both the RISM and lattice theory appear to be quite similar.

The lattice cluster theory has the one benefit, despite its greater oversimplification of reality, that a single calculation *simultaneously* provides expressions for the thermodynamic properties of polymer–solvent and polymer–polymer systems for *all* molecular weights, monomer and solvent structures, and compositions, whereas integral equation methods are inherently numerical and require separate computer calculations for each value of all these aparameters. Thus, the determination of coexistence curves from RISM methods would require large amounts of computer time, while their derivation from the analytical expressions in the tables here is computationally trivial. In addition, the calculations presented here apply to polymer–solvent systems that are currently not amenable to RISM methods because of the inherent concentration dependence of the intramolecular polymer correlation functions in such systems. On the other hand, the RISM methods yield structure factors that currently cannot be obtained from the lattice cluster theory. Continuum models provide more realistic descriptions than do lattice models for equations of state for very short polymers.[29] However, methods have been suggested for rectifying some of these deficiencies of lattice models,[29] and it remains to be seen whether lattice or continuum approaches will be the most useful for treating data for actual polymer systems. The above comparison of lattice and continuum approaches is designed to stress the limitations of the current theories and to emphasize the complementary nature of these different methods.

Schweizer and Curro[32] note some differences between their calculated effective interaction parameter χ_{eff} and that obtained from the lattice theory by Pesci and Freed. While the latter calculations are corrected in the tables given here, several differences with Schweizer and Curro might appear to remain. However, it must be noted that the present tables refer to incompressible polymer–polymer systems, while Schweizer and Curro perform calculations for compressible polymer blends. Monte Carlo calculations for symmetric ($M_1 = M_2$) blends of lattice polymers by Sariban and Binder[34] appear to display a composition-dependent χ in conformity with the work of Schweizer and Curro. A difficulty with the data of Sariban and Binder is that χ_{eff} is presented only along the coexistence curve, and thus the data applies to blends at widely differing temperatures, a variation that could impart the composition dependence to χ_{eff}. Our lattice cluster theory for incompressible blends of very long polymers shows the athermal limit entropy of mixing to be composition independent, but, as will be presented elsewhere, that is no longer true for compressible blends. It likewise does not apply to the hard-sphere model calculations of Schweizer and Curro, which involve compressible blends. Compressible blend lattice cluster theory computations for the symmetric system of Sariban and Binder (both species linear chains, $M_1 = M_2 = 32$, $\epsilon_{11} = \epsilon_{22} = 1$, $\epsilon_{12} = 0$) exhibit a χ_{eff} with a significant parabolic composition dependence[35] that mirrors the variation obtained in the Monte Carlo calculations. Thus, it appears that the general conclusions of the lattice and continuum theories coincide with the composition dependence of χ_{eff}.

Although we presently do not have the Monte Carlo simulations that are necessary to check the accuracy of the energies of mixing and coexistence curves for incompressible polymer blends, there is reason to believe that these should be more easily describable than the polymer–solvent case because of the lower disparity of molecular volumes in the former than in the latter case. The polymer blend coexistence curves are much more symmetrical than the highly asymmetric polymer–solvent curves. Consequently the chemical potentials of the coexisting polymers are not extremely small and therefore are not so sensitive to minor errors as in the polymer–solvent case. Thus, we anticipate that our predictions in the tables should be even more accurate for incompressible blends than the demonstrated accuracy for polymer–solvent systems.

Acknowledgment. This research is supported, in part, by NSF Grant DMR89-19941 and a grant from the donors

of the Petroleum Research Fund, administered by the American Chemical Society. We are grateful to Moungi Bawendi, Jack Douglas, and Shawn Huston for comments on the manuscript.

Appendix A: Interaction Energy Diagrams and Their Evaluation

The diagrams for the partition function Z of (3.3) may contain both correlating bonds and interaction lines. Some of the diagrams of first order in ϵ are represented in Figure 3. Their evaluation proceeds as in previous papers,[6,18] but here they are evaluated without approximation for an incompressible binary system with structured monomers and/or solvent molecules. The derivation of the ϵ diagram rules follows within the algebraic representation of section 3 in a fashion paralleling that presented in section 2 for the athermal limit entropy. The major considerations are the following: Consider first the linear term in f_{kl} in (3.5). Because the factor of $\delta(i,j+\beta)$ implies that $i \neq j$, the sum $\sum_{i>j} = (1/2)\sum_{i,j}$. The two indices i and j in this summation may either differ or coincide with any of the site indices for the correlating bonds from contributions to the expansion (2.11) in (2.7) and (3.3). It is, therefore, necessary to count the number of possible ways of selecting the sites involved in the correlating bonds and in the interaction lines from among the monomers and solvent molecules present in the system. This counting factor is contained in the analogue of γ_D as generalized to the energy diagrams in ref 6. Here we illustrate the counting process for the higher order ϵ diagrams.

The extended mean-field energy diagrams through order ϵ^4 are presented in Figure 4. These diagrams contain only interaction lines. The subscripts designate the order in the Mayer f function, $f = \exp(\epsilon) - 1$, and we consider them for the case of a polymer–solvent system. Generalizations to compressible blends are possible by the present methods, but the computations are more lengthy and will be presented elsewhere. Because the system is assumed to be incompressible, Madden[14] has demonstrated that ϵ may be taken to be the polymer–polymer interaction, while the polymer–solvent and solvent–solvent interactions vanish. (This is because excess thermodynamic quantities for the incompressible system depend only on the single interaction parameter ϵ of (2.1)). The summation indices in (3.5) may be converted to unrestricted summations over all lattice sites, provided that factors of $^1/_2$ are introduced as above, that terms are included in which the same lattice site appears in different delta factors in (3.5), and that symmetry factors are included. For instance, the order f^2 term of (3.5) may have contributions where none of the four lattice site indices coincide or one lattice site is common between the two δ factors. These contributions correspond, respectively, to diagrams A_2 and B_2 of Figure 4. The counting factors from the summation of (3.5) are represented in Table V, where in diagram A_2 there is now a sum over $i \neq j \neq i' \neq j'$, while in B_2 there is a sum over $i(\equiv j) \neq i' \neq j'$. The $^1/_2$ for A_2 arises because of the equivalence of the two f factors. Higher order counting factors follow similarly.

The values of diagrams A_1, A_2, and B_2 follow according to the general rules for ϵ diagrams, described in refs 6 and 18, that may be read without reference to the field theory used in those papers for the derivation of the rules given there. The series (3.5) contains the Mayer f function of (3.2), and these f functions are further expanded in a power series in ϵ, retaining terms through a given order. It is possible to represent this power series expansion by the introduction of additional diagrams such as diagram C_2 of Figure 4, which is equal to the ϵ^2 portion arising from the f function expansion of diagram A_1. In higher orders, it is convenient to retain the f function form, eliminate the extra diagrams like C_2, and then perform the ϵ expansion of the f functions. The resultant expressions for diagrams A_1, A_2, and B_2 are presented in Table V, where R_{21}' designates the z^{-1} portion of the contracted diagram R_{21} of Table III of Nemirovsky et al.[15] The $\mathbf{q} = 0$ portion from use of (2.5) in the δ function of (3.5) is the sole contribution to diagram A_1, but as noted above, the $\mathbf{q} = 0$ terms in higher order energy diagrams appear to cancel order by order in ϵ. Thus, the ϵ^2, ϵ^3, and ϵ^4 diagrams of Figure 4 are evaluated by retaining the $\mathbf{q} \neq 0$ portions only. This makes their evaluation formally identical with that for the entropy diagrams, except for the counting prefactor γ_D that differs for the two cases as described in ref 6 and below. The elimination of diagrams, such as diagram C_2, and the retention only of $\mathbf{q} \neq 0$ contributions enormously simplifies the evaluation of the ϵ diagrams and has aided in evaluating the higher order terms.

Diagrams A_2, B_2, and C_2 have leading contributions in $\epsilon^2 z^2$ that cancel among this class of diagrams, so Table V only presents that portion of the diagram that survives after cancellation of these terms as well as the cancellations involved in formation of cumulants. The formation of cumulants cancels all contributions from individual diagrams that scale as higher powers than N_l. Table V also omits terms in N_l^0 that vanish in the thermodynamic limit. The removal of the $\epsilon^2 z^2$ and higher order contributions involves partial cancellation by the $\mathbf{q} = 0$ terms from A_2 and B_2 in which one or both of the interaction lines have $\mathbf{q} = 0$. Similar cancellations occur in higher orders where all terms in $\epsilon^3 z^3$, $\epsilon^3 z^2$, $\epsilon^4 z^4$, $\epsilon^4 z^3$, and $\epsilon^4 z^2$ are cancelled. The algebra is quite tedious, and a great deal of simplification is otained by droping these terms and all $\mathbf{q} = 0$ contributions from interaction lines, whereupon the evaluation of the ϵ diagrams proceeds as readily as with the athermal limit packing entropy diagrams.

Table V follows the notation of ref 15 in which the diagram value D_B is written as

$$D_B \equiv \alpha d_B \tag{A.1}$$

where α depends on the number of sites, n_v, in the diagram through

$$\alpha = [N_l(N_l - 1)\cdots(N_l - n_v - 1)]^{-1} \tag{A.2}$$

The combinatorial factor α_D of (2.13) for the ϵ diagrams of Figure 4 is

$$\alpha_D \equiv s[Mn_p(Mn_p - 1)\cdots(Mn_p - n_v - 1)] \tag{A.3}$$

where s is the diagram symmetry factor from Table V. Then, after all the cancellations described above, d_B is equal to $f^n(z/N_l)^n$ multiplied by the contracted diagram listed under the column d_B factor in Table V.

The sum of the ϵ^2 diagrams A_2, B_2, and either C_2 or the ϵ^2 part of A_1 yields $(\epsilon^2/4)z\varphi^2(1-\varphi)^2$ in agreement with Bawendi and Freed.[18] The ϵ^3 and ϵ^4 diagrams of Figure 4 are also evaluated in Table V, where R_{31}' is the order z^{-2} portion of the contracted diagram R_{31} from Table III of ref 15, and R_{42}' and R_{46}' are the order z^{-3} parts of R_{42} and R_{46}. Reference 15 does not provide the z^{-3} contributions to R_{42}, and R_{46} is a new contracted diagram that is presented in Figure 4. (The results in ref 15 are independent of these terms.) The full expressions for these contractions are as follows:

$$R_{31} = (N_l^4/z^2)[1 - (3z/N_l) + 2(z/N_l)^2] \tag{A.4}$$

$$R_{42} = 3(N_l^5/z^2)[1 - z^{-1} - (z^2/3N_l)] \quad \text{(A.5)}$$

$$R_{46} = (N_l^5/z^3)[1 - (z/N_l)]^3 \quad \text{(A.6)}$$

In order to obtain (A.4)–(A.6), care must be taken in evaluating contracted diagrams as follows: A constraint $\sum_{\mathbf{q}_1,\mathbf{q}_2,\mathbf{q}_3\neq 0}\delta(\mathbf{q}_1,\mathbf{q}_2+\mathbf{q}_3)$ requires imposition of the condition $\mathbf{q}_2 \neq \mathbf{q}_3$ on the sum over $\mathbf{q}_2$ and $\mathbf{q}_3$. The leading contributions of order ϵ^n emerge from individual diagrams as $(\epsilon z)^n$, while the overall contributions begin as $\epsilon^n z$, so there is extensive cancellation of the leading portions as n increases, a cancellation that provides a useful check on the calculations. Fortunately, the present comparison with Monte Carlo simulations finds these higher order ϵ terms to be rather insignificant beyond ϵ^2.

References and Notes

(1) *Polymer Handbook*; Brandup, J., Immergut, E. H., Eds.; Wiley: New York, 1975.
(2) Freed, K. F. *Encyclopedia of Polymer Science and Engineering*; Wiley: New York, 1989; Vol. 15.
(3) Panayiotou, C. G.; Vera, J. H. *Polym. J.* **1982**, *14*, 681.
(4) Kumar, S. K.; Suter, U. W.; Reid, R. C. *Ind. Eng. Chem. Res.* **1987**, *26*, 2542. Panayiotou, C. G. *Macromolecules* **1987**, *20*, 861. Koningsveld, R.; Kleintjens, L. A.; Leblans-Vinck, A. M. *J. Phys. Chem.* **1987**, *91*. 6423.
(5) Madden, W. G.; Pesci, A. I.; Freed, K. F. *Macromolecules* **1989**, *23*, 1181.
(6) Pesci, A. I.; Freed, K. F. *J. Chem. Phys.* **1989**, *90*, 2003.
(7) Pesci, A. I.; Freed, K. F. *J. Chem. Phys.* **1989**, *90*, 2017.
(8) Dickman, R.; Hall, C. K. *J. Chem. Phys.* **1986**, *85*, 3023. See also: Hertanto, A.; Dickman, R., preprints.
(9) Flory, P. J. *J. Chem. Phys.* **1941**, *9*, 660; **1942**, *10*, 51. Flory, P. J. *Principles of Polymer Chemistry*; Cornell University: Ithaca, NY, 1953.
(10) Huggins, M. L. *J. Chem. Phys.* **1941**, *9*, 440; *J. Phys. Chem.* **1942**, *46*, 151; *Ann. N.Y. Acad. Sci.* **1943**, *44*, 431.
(11) Mayer, J. E.; Mayer, M. G. *Statistical Mechanics*; Wiley: New York, 1940.
(12) Guggenheim, E. A. *Proc. R. Soc. London Ser. A* **1944**, *183*, 203; **1944**, *183*, 213. Guggenheim, E. A. *Mixtures*; Oxford University Press: Oxford, 1952.
(13) Freed, K. F.; Bawendi, M. G. *J. Phys. Chem.* **1989**, *93*, 2194.
(14) Madden, W. G. *J. Chem. Phys.* **1990**, *92*, 2055.
(15) Nemirovsky, A. M.; Bawendi, M. G.; Freed, K. F. *J. Chem. Phys.* **1987**, *87*, 7272.
(16) Freed, K. F. *J. Phys. A* **1985**, *18*, 871.
(17) Bawendi, M. G.; Freed, K. F.; Mohanty, U. *J. Chem. Phys.* **1986**, *84*, 7036; **1987**, *87*, 5534. Bawendi, M. G.; Freed, K. F. *J. Chem. Phys.* **1986**, *85*, 3007.
(18) Bawendi, M. G.; Freed, K. F. *J. Chem. Phys.* **1988**, *88*, 2741.
(19) Kubo, R. *J. Phys. Soc. Jpn.* **1962**, *17*, 1100.
(20) Freed, K. F.; Pesci, A. I. *Macromolecules* **1989**, *22*, 4048.
(21) There is a minor polydispersity in the Monte Carlo sample ($M_w/M_n = 1.085$), which Madden et al.[5] show is inconsequential except on the dilute side of polymer–solvent coexistence curve.
(22) Miller, A. R. *Proc. Cambridge Philos. Soc.* **1942**, *38*, 109; **1943**, *39*, 54.
(23) de Gennes, P.-G. *Scaling Concept in Polymer Physics*; Cornell University Press: Ithaca, NY, 1979. Freed, K. F. *Renormalization Group Theory of Macromolecules*; Wiley: New York, 1987.
(24) In ref 5 Madden et al. find that the best agreement with simulations is obtained when the first-order Guggenheim free energy of mixing is supplemented with the second-order term from the EMF. The coexistence curve obtained from the present second-order LCT and shown in Figure 8 is superior to the coexistence curve obtained from the earlier jerry-built equation constructed by Madden et al.[5]
(25) The correct coefficient $N_{1,2}$ for type d geometry, depicted in Figure 1 and in ref 6, is $N_{1,2} = (N - 2)(3N - 5)$.
(26) Freed, K. F. *J. Chem. Phys.* **1988**, *88*, 5871. Dudowicz, J.; Freed, K. F. *Macromolecules* **1990**, *23*, 1519.
(27) Binder, K., preprint. Similar behavior is reported by Fishman (*Phys. Rev. Lett.* **1989**, *63*, 89) for granuled superconductors.
(28) Bawendi, M. G.; Freed, K. F. *J. Chem. Phys.* **1987**, *86*, 3720.
(29) Dickman, R.; Hall, C. K. *J. Chem. Phys.* **1986**, *85*, 4108.
(30) Dee, G. T.; Walsh, D. J. *Macromolecules* **1988**, *21*, 815.
(31) Flory, P. J. *Discuss. Faraday Soc.* **1970**, *49*, 7.
(32) Schweizer, K. S.; Curro, J. G. *J. Chem. Phys.* **1989**, *91*, 5059.
(33) Curro, J. G.; Schweizer, K. S.; Grest, G. S.; Kremer, K. *J. Chem. Phys.* **1989**, *91*, 1357.
(34) Sariban, A.; Binder, K. *J. Chem. Phys.* **1987**, *86*, 5859.
(35) Dudowicz, J.; Freed, K. F., unpublished work.